UNIVERSITA' DEGLI STUDI DI MILANO

PhD Course, XXX Cycle

Ricerca Biomedica Integrata

The expression of the rare caveolin-3 variant T78M alters cardiac ion channels function and membrane excitability.

Tutor: Prof. Di Francesco Dario

Coordinator: Prof.ssa Sforza Chiarella

Bonzanni Mattia

Matr. R10851

‘Electrophysiologists never die, they only depolarize.’

Silvio Weidmann

PREFACE

The identification of new molecular insights always drove the research. Data from genetic, molecular biology and biochemistry suggest new directions, open new fields and lead to new discoveries. The significance of these data is, in certain situation, difficult to envision. In this view, physiology could represent a reasonable read-out of the overall complex modifications inside the cell. In particular, electrophysiological analysis could shed light on both physiological and pathological conditions in excitable cells, where ion channels, cellular microenvironment, transcription factors and accessory proteins shape the electric profile. In my PhD, I mainly used this approach to test the effect of mutations found in patients affected by arrhythmic disorders (cardiac arrhythmia and epilepsy) and of exercise training on the electrical activity in the heart. In particular, I performed the following projects:

- Electrophysiological characterization of the biophysical properties of the hHCN1 L157V mutation found in a patient affected by idiopathic generalized epilepsy. A genetic panel testing more than 150 genes previously associated with the epileptic phenotype, failed to detect any other mutation over the L157V HCN1. I tested the effect of this mutation in a heterologous cell system (CHO cells) as well as in a simple neuronal environment, the neonatal rat cortical cells. In both cellular systems, the mutation affects the current density (-50% and -80% in CHO and neurons, respectively) in a dominant way over the WT isoform. The loss-of-function of the HCN1 current induced, *in vitro*, an increased excitability in cortical neurons, pointing out that the L157V could establish a susceptible environment more prone to epileptogenic events.
- Analysis of the miRNA profile in response to chronic endurance training. I found that, in a mouse model of endurance training, the cardiac miRNA profile was affected in a regional-dependent manner. Moreover, some of these miRNAs were able to modulate the spontaneous firing rate of neonatal rat ventricular myocytes similarly to the modification found in the single cell isolated from the pacemaker region in trained mice. It is important to mention, moreover, that the cardiac levels of miR-1 and miR-499a, muscle specific miRNAs modulated in the mouse model of training and able to affects the firing rate, correlate with their circulating levels and were modified in the plasma of human ultra-endurance athletes as well, suggesting a potential conserved pathway.

- Characterization of the impact of the T78M cav-3 variant found in a cohort of arrhythmic patients. This variant induces modification of several ionic currents leading to a pro-arrhythmogenic profile. This project is described in the present work.

In the present study, I describe the project concerning the analysis of the T78M cav-3 variant. This variant has been previously associated with cardiac and skeletal disorders, but recently its role in the onset of arrhythmic diseases was questioned. A better understanding of the molecular effect of this variant could be helpful to settle its impact in a cardiac context. For this reason, I decided to present this work as my PhD thesis since these data could re-open the discussion on this variant and better define its impact in these life-threatening conditions.

The *leitmotiv* of these projects is the identification of the causes underlying the pathophysiological modification of excitable cells; they clearly showed that ion channels, membrane proteins and post-transcriptional factors are key player in defining the electrical environment of a cell.

Index

INTRODUCTION

The multiple faces of caveolae.

Signaling activity of biomembranes strictly depends on geometric parameters such as surface area and curvature; alongside the shape of the membrane, the inhomogeneity of this curvature is critical in defining protein association and hence signaling[1]. In many cell types, specialized highly hydrophobic plasma membrane subdomains known as caveolae play a key role in several cellular processes. These structures are small clathrin-free omega-shaped (50-100 nm) invaginations of the plasma membrane highly enriched in sphingolipids and cholesterol[2]. However, the definition of caveolae has been expanded to also include vesicles detached from the plasma membrane, associated in group as grasp-like clusters or rosettes[3]. It is important to note that, even if caveolae shares common aspect with lipid rafts (planar rafts with high cholesterol and sphingolipids content) such as the main lipid composition, they are distinct structures. In fact, it has been reported that several proteins resides specifically either in lipid rafts or in caveolae[3]. In particular, the localization of the caveolin proteins into caveolae distinguished them from lipid rafts. Indeed, caveolins are specific markers of the caveolar structure.

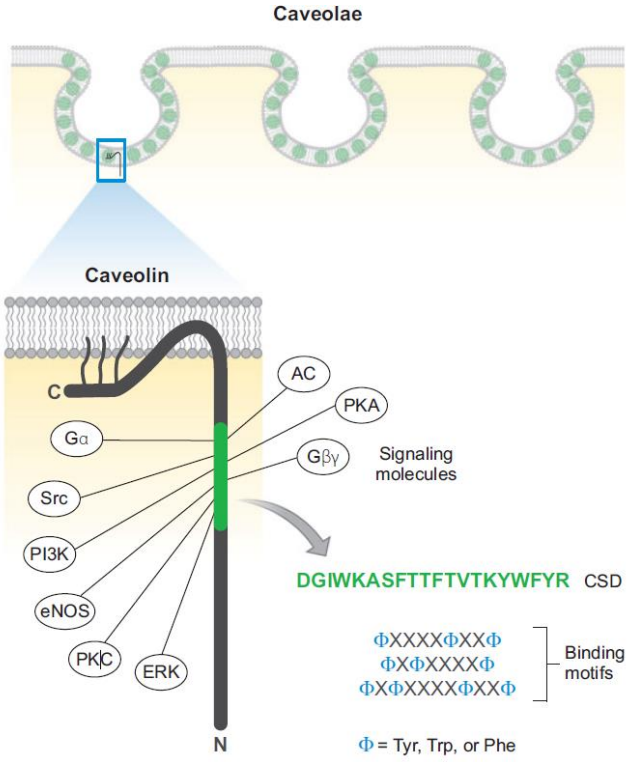

Figure. 1 Caveolin structure from Patel et al., 2008

Molecular cloning has identified three different isoforms of caveolin (cav): cav-1, cav-2 and cav-3. They are 18-24 kDa proteins characterized by a "hairpin-like" topology (Fig. 1) with an N-terminal cytoplasmic domain containing the so called "scaffold domain", which is crucial in the protein-protein interactions[4]. The sequences of cav-1 and cav-3 share a high degree of identity, whereas cav-2 is the most divergent isoform[5]. Despite this deviation, cav-2 is detected selectively in cav-1 expressing cells. Indeed, cav-1 and -2 act in concert and they are most abundantly expressed in adipocytes, endothelial cells, type I pneumocytes and fibroblastic cell types, whereas the expression of cav-3 is considered muscle-specific (smooth, skeletal and cardiac muscles). This peculiar differential cellular distribution points out that cav-1 and -3 proteins, in spite of their high degree of identity, might possess distinct functions. Importantly, the ablation of both cav-1 and cav-3 is sufficient to inhibit the formation of caveolae, confirming their role as essential constituents in the biogenesis of caveolar domains[6]. Together with caveolin, the members of the cavin protein family (cavin-1, -2, -3 and -4) aid in the generation of mature caveolae fostering the oligomerization of caveolin proteins. Cavins are cytoplasmic proteins with amino-terminal coiled-coil domains that form large heteromeric complexes and assist caveolin in the curvature of the plasma membrane. The predisposition of caveolin proteins to form oligomers, as well as the presence of cholesterol, are essential contributing factor to the formation of the caveolar domains. Indeed, caveolae synthesis is a complex, stepwise assembly process which requires several distinct molecules[7](Figure 2). Caveolins are synthetized in the endoplasmic reticulum and rapidly undergoes the first stage of oligomerization generating oligomers formed by 7 to 14 caveolin monomers (8S-cav). After the exportation of these oligomers from the endoplasmic reticulum to the Golgi complex, cholesterol crystalized and assist to the 70S-caveolin oligomers formation combining 18-25 8S-cav structures. Indeed, cholesterol plays a critical role in the biogenesis, integrity and function of caveolae; in fact, its depletion leads to the disruption of the mature caveolar structure and prevent their genesis. Prior the insertion of the mature caveolar structure in the plasma membrane, both palmytoilation and cavin insertion processes are performed.

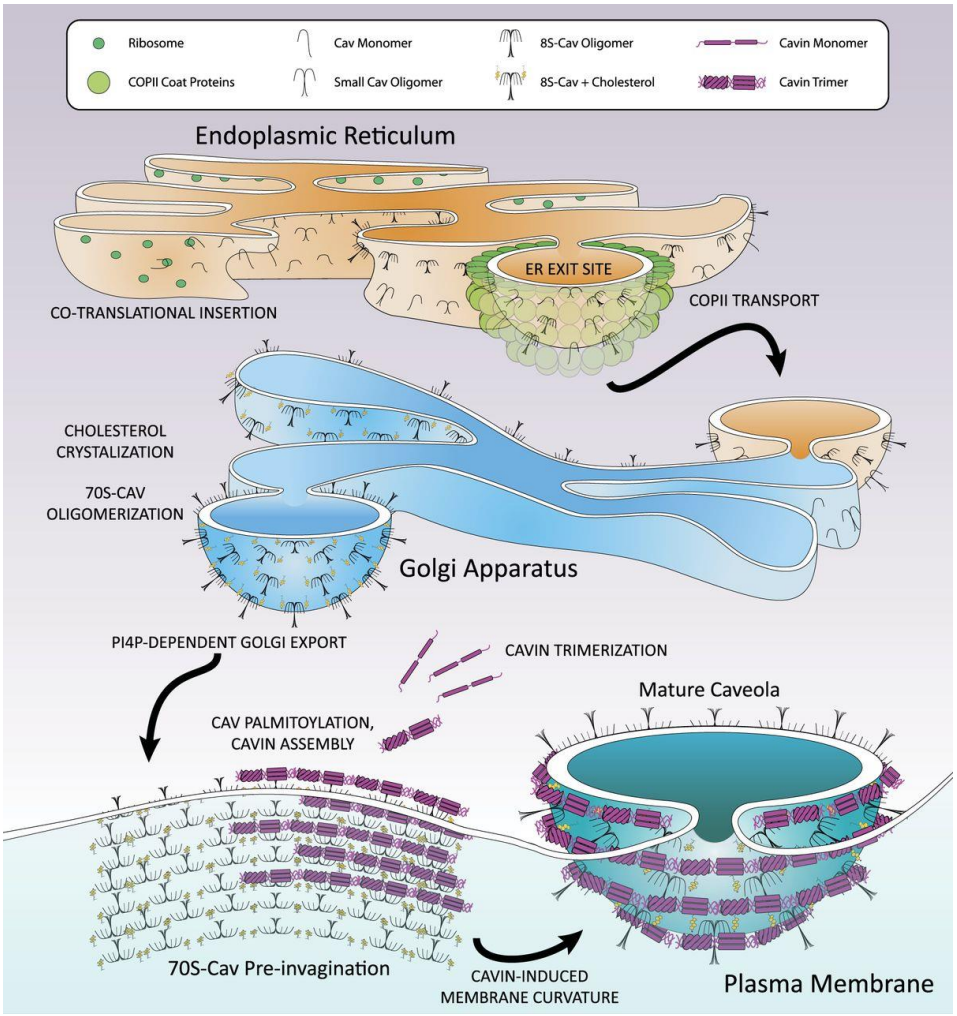

Figure. 2 Genesis of the caveolar mature domains from Busija et al., 2017

Interactions between caveolins, cavins, lipids, and other proteins create an unique protein, lipid, and lipoprotein cellular microenvironment. Indeed, caveolae is an attractive way to segregate or integrate certain pathways in microdomains of the plasma membrane. Moreover, caveolae has been implicated in several physiological processes behind membrane trafficking and compartmentalization. For example, despite they were initially identified as almost static structure, caveolae participate in cell transport events such as endocytosis, transcytosis and pinocytosis[2]. Moreover, caveolar structures play a critical role not only as a transducer of the mechanical stimuli into chemical ones, but also participate in the cell migration processes. This modulation of the cytoskeleton is a consequence of the association between caveolae and several components of the cytoskeletal apparatus such as actin filaments, microtubules and intermediate filaments[5]. It is also important to mention that they have an important role in the homeostasis of cholesterol in the cell. Mainly, the influence of caveolae has been characterized extensively in signaling transduction processes; this is referred to as the "caveolae signaling hypothesis".

The protein residing in the caveolar structure could bind directly the caveolin proteins thanks to the presence of a region known as caveolin binding domain (CBD). This region recognizes the so-called caveolin scaffolding domain (CSD) on the caveolin proteins, in particular cav-1 and cav-3. Caveolae, indeed, appeared to serve as signaling platforms for several different proteins, from signaling molecules, to receptors and ion channels. For example, caveolae generated by cav-1 compartmentalize G-protein subunits, receptor and non-receptor tyrosine kinases, endothelial nitric oxide synthase (eNOS), and small GTPases, while in the caveolae generated by cav-3 were found β-adrenergic receptors, protein kinase C isoforms, G proteins, Src-family kinases, multiple components of the dystrophin-glycoprotein complex and many ion channels[8].

Much insight into caveolar function has been gained thanks to the generation of caveolin null mice. Interestingly, the absence of caveolae in cav-1, cav-3 and double cav-1/3 KO mice did not lead to developmental abnormality nor lethality[9]. In particular, cav-1 KO mice had an increased cell proliferation, suggesting a tumor suppressor activity of cav-1. Moreover, cav-1 KO mice develops cardiac hypertrophy. The absence of cav-3, on the other hand, leads to mild degenerative processes in the skeletal muscles without affecting the dystrophin-associated complex and promote the development of a progressive cardiomyopathy[10]. Furthermore, both dihydropyridine receptor-1 α and ryanodine receptor were mislocalized in the T tubules, suggesting a pivotal role of cav-3 isoform in the proper assembly of this structure. The double cav-1/cav-3 KO mouse [11] develops severe cardiomyopathy promoted by a dramatic increase in left ventricular thickness with a significant decrease in fractional shortening. Moreover, histological analysis of Cav-1/3 double KO hearts revealed also disorganization and degeneration of the cardiac myocytes, as well as chronic interstitial fibrosis and inflammation. Despite many signaling processes are blunted and cardiac defects are reported in all KO mice models, compensatory mechanisms seems to counterbalance the absence of the caveolae structures in these transgenic mice.

Ion channels residing in caveolae.

Among proteins residing in caveolae, different subtypes of ion channels are present. Ion channels are a large family of molecules that are influenced by the subcellular microenvironment set by the caveolae. Indeed, a critical factor for understanding the regulation of ion channels is their precise subcellular localization, which is instrumental in the regulation of the underlying currents[12]. Ion channels are transmembrane proteins that conduct ionic currents across the plasma membrane. In excitable cells, they play a key in the

modification of the transmembrane potential and their activity is fundamental in the generation of membrane excitability in many cell subtypes. The peculiar lipid environment present in the caveolae can directly affect the biophysical properties of ion channels; similarly, the compartmentalization of the signaling molecules able to specific regulate ion channel activity determines a highly localized control of ionic currents. Furthermore, the ability of caveolae to traffic the proteins to the plasma membrane regulates the availability of ion channels, and thus the current density[12].

Voltage-gated sodium channel.

The voltage-gated sodium channel $Na_v1.5$, encoded by *SCN5A*, was one of the first channels detected in caveolae. This channel is responsible for the initial upstroke phase of the action potential of both atria and ventricles and contributes to propagation of electrical impulses in the heart. The characteristics of I_{Na} current are influenced by the presence of β-adrenoreceptors (βAR) in caveolae. In particular, βAR stimulation induced an increase in current amplitude through a PKA-dependent phosphorylation of the channel and by direct $G_{\alpha s}$ modulation[12].

L-type calcium channel.

L-type calcium channels $Ca_v1.2$ (*CACNA1C*) are voltage-gated channels critical for the influx of Ca^{2+} able to trigger excitation-contraction coupling and they contribute to the plateau phase in myocytes of the working myocardium. In adult mammalian ventricular myocytes, L-type channels have been localized to both surface and T-tubular sarcolemma. Moreover, they are the major contributors of the upstroke phase in sinoatrial node cells. Some, but not all, $Ca_v1.2$ resides in the caveolae[13]. Most importantly, various proteins involved in the cAMP/PKA signaling (i.e. β_2 ARs, AC5/6, Gs, Gi, PP2A, and the type II R subunit of PKA), which are able to influence I_{CaL}, reside in the caveolae[14] and many of these have been tied to $Ca_v1.2$ through protein-protein interaction[13]. Functionally, the chemical depletion of cholesterol, which disrupts caveolae, led to an enhancement of the L-type calcium current because of the disruption of the inhibitory effect exerted by cav-3 on both β_2-AR and adenylyl cyclase activity[15]. These results indicate that the caveolar domain is relevant in the proper maintenance of the β-AR-dependent modulation of $Ca_v1.2$ channels without affecting calcium current density.

Potassium channels

In cardiomyocytes, several potassium channels are present and divided in voltage-gated (K_v) and inward rectifier (K_{ir}) channels with peculiar cardiac sub-localization and unique gating properties. The K_v family includes I_{to}, I_{Kur}, I_{Kr}, and I_{Ks}, whereas I_{K1}, I_{KACh}, and I_{KATP} belongs to the K_{ir} family. The main tasks of potassium channels are to maintain the resting membrane potential (in working myocardium cells) and to repolarize the cell during the action potential. Some potassium channels are localized out of the caveolar domains, such as $K_v11.1$ (I_{Kr}), while $K_v1.5$ (I_{Kur}), $K_{ir}2.1$ (I_{K1}) and $K_{ir}6.2$ (I_{KATP}) have been specifically identified in the caveolae. $K_v11.1$, even if is present in low-density membrane fractions, does not co-immunoprecipitate with cav-3[16]. Nevertheless, this channel is sensible to cholesterol depletion, indicating a connection between lipid composition and the channel activity. The $K_v1.5$ channel is responsible for the ultrarapid component of the delayed rectifier potassium current, the I_{Kur}. The channels possess also an inactivation state and they are involved in the initial phase of the repolarization of the atrial action potential. Despite the localization of $K_v1.5$ channels is under debate[12], $K_v1.5$ seems to reside in both caveolar and non-caveolar domains. However, McEwen *et al*[17] clearly demonstrated that cav-3 is able to recruit $K_v1.5$ channels from non-raft regions thanks to the formation of a tripartite complex with SAP97[18]. Moreover, the caveolar localization of the $K_v1.5$ channels affects the gating properties of the channel. Indeed, the disruption of caveolae led to a modification of the kinetic parameters of I_{Kur} in the HEK cellular system[19].

Hyperpolarization-activated cyclic nucleotide–gated (HCN) channels.

HCN channels conducts a mixed cationic inward current called funny current (I_f), which is one of the main current that contribute to cardiac automaticity in the sinoatrial node, the pacemaker region of the heart[20]. HCN channels are activated upon hyperpolarization of the membrane[21] as well as in response to the binding of cyclic nucleotide such as cAMP[22]. Among the four isoforms of HCN channels (HCN-1, -2, -3 and -4), HCN4 is the main one expressed in nodal cells. HCN4 were demonstrated not only to specifically localize in the low density membrane fractions, but also to be functionally influenced by cav-3. The disruption of caveolar domain induced a rightward shift of the activation curve of HCN4; in addition, the depletion of cholesterol alters the channel kinetics[23]. The shift of the activation curve to more depolarized potentials after the disruption of the caveolae determined a faster firing rate of spontaneous action potentials in sinoatrial node cells. Furthermore, the caveolar integrity is crucial in the β_2-AR-dependent modulation of the f-channels, and hence firing rate in the

sinoatrial node[24]. The critical modulation of HCN4 by caveolae is a consequence of the direct binding of this channel to cav-3. Indeed, a caveolin-binding motif is present in the sequence of the HCN4 channel, and the disruption of this binding domain led to an accumulation of the channel in the Golgi complex, indicating a close relation between the ability of HCN4 to bind cav-3 and its proper translocation to the membrane[25].

Caveolinopathies.

Caveolinopathies are a heterogeneous group of muscle diseases that arise from mutation in the *CAV3*. Indeed, *CAV3* is the only gene known to cause caveolinopathies[26]. A clear genotype-phenotype correlation cannot be traced in such pathology and both skeletal muscle and cardiac defects were associated with *CAV3* mutations[27], as visible in Figure 3, in which the same mutation was detected in patients affected by different phenotypes. Most of the caveolinopathies are inherited in heterozygosis with an autosomal-dominant inheritance, and only few autosomal recessive *CAV3* mutations were reported. To date, the skeletal muscle phenotypes associated with *CAV3* mutations are: limb girdle muscular dystrophy 1-C (LGMD), HyperCKemia (HCK), rippling muscle disease (RMD) and distal myopathy (DM). Together with the skeletal muscle phenotype, also cardiac defects were associated with *CAV3* mutations, even if the cardiologic component is less frequent or underdiagnosed. In particular, were reported patients carrying CAV3 mutations and affected by familial hypertrophic myopathy (FHM), Long-QT syndrome (LQTS) and some cases of sudden infant death syndrome (SIDS)[28].

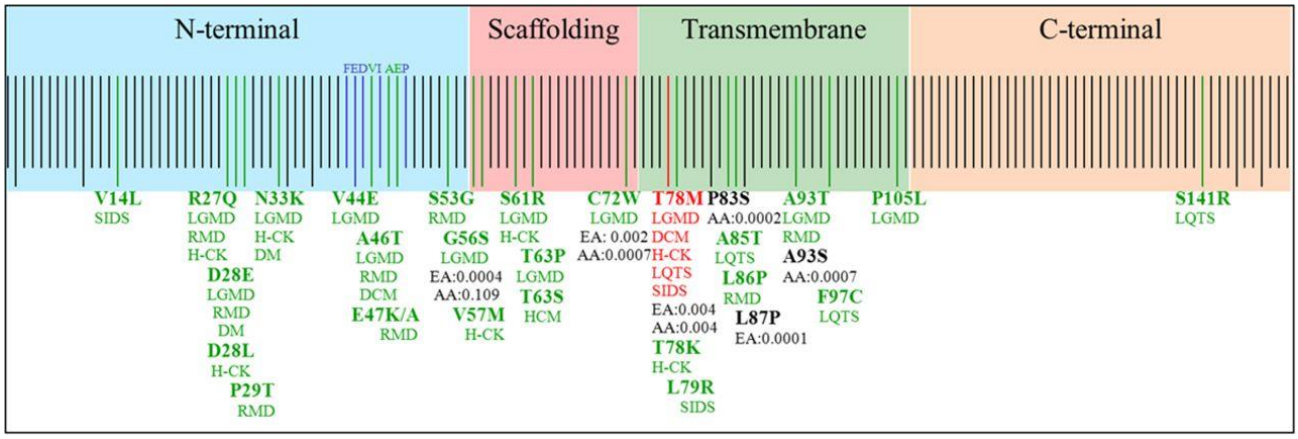

Figure. 3 Hedley et al., 2013

Caveolinopathies could be considered as a "clinical continuum", since many patients showed an overlap of several skeletal muscle phenotypes. Among the *CAV3* mutations identified until

now, T78M was the most common substitution [27-29] and it has been associated with both skeletal and cardiac diseases.

T78M cav-3: a variant or a mutation?

The 233C >T variant introduce the substitution of a methionine in place of a threonine in position 78 (T78M) of the cav-3 protein. It has been identified in patients with RMD, proximal myopathy, LQTS, idiopathic hyperCKemia, and SIDS[28,30-32]. A single patient homozygous for the T78M cav-3 was reported and he was affected by dilated cardiomyopathy, hyperCKemia and proximal myotonia[33]. The localization of T78M cav-3 was controversial. Indeed, in COS-7 cells transfected with either the WT or T78M cav-3, both isoforms reached the plasma membrane[33]; in contrast, muscle biopsies of T78M cav-3 patients revealed a faint plasma membrane localization [32]. Behind the identification of the T78M cav-3 in the above-mentioned spectrum of diseases, few studies reported also the impact of the mutation on the ionic channel activity, hence providing evidence of functional alterations induced by the mutated cav-3. Cronk and colleagues[31] found V14L, T78M and L79R cav-3 in a cohort of sudden infant deaths and T78M in 3 cases of LQTS over 1000 control alleles. They discovered that the co-expression of the T78M cav-3 with $Na_v1.5$ in HEK cells induced a persistent late-sodium current (late I_{Na}), which generates a "gain-of-function" of the I_{Na} compatible with the LQTS clinical phenotype (characterized by a prolonged QT interval on the electrocardiogram and sudden cardiac death secondary to cardiac arrhythmias). Vaidyanathan and colleagues[34] then demonstrated that T78M cav-3 is also able to significantly reduced the I_{K1} current in HEK cells. The loss of I_{K1} current, which is important in the proper maintenance of the resting membrane potential as well as in the repolarization of the action potential, was previously associated with different types of LQTS. These *in vitro* results, even if performed overexpressing the proteins in a heterologous cellular system, point out to a pro-arrhythmogenic role of T78M cav-3. Lately, however, genetic analysis questioned the potential pathogenic role of the T78M cav-3. In particular, Refsgaard *et al* [35] and Andreasen and colleagues [36] identified the T78M cav-3 in healthy controls and in a cohort of patients affected by LQTS or in case of SIDS with a similar prevalence, accordingly to the data from the Exon Sequencing Project. In agreement, Spadafora *et al*[37] reported the T78M cav-3 as a common polymorphism in South Italy. To date, the literature on the T78M cav-3 has neither clarified the impact of this mutation on membrane excitability, nor its role in the insurgence of arrhythmic diseases.

AIM OF THE WORK

Arrhythmias are the most common electrical disturbances of the heart. Even if the etiology is complex and multifactorial, many genetic loci are associated with the insurgence of arrhythmic diseases. The microenvironment is able to shape and coordinate electric phenomena, and structural proteins such as caveolin are well-recognized modulators of ion channel activity. Mutations on *CAV3* were identified in patients affected by both skeletal and cardiac pathologies, and among them, the most common variant is the T78M cav-3. In literature, the effect of the T78M variant remains unresolved and its pathogenic role is under debate; some *in vitro* studies suggest a pro-arrhythmogenic behaviour induced by T78M cav-3, whereas genetic studies argued against its causative effect in cardiac dysfunctions. Considering that many cardiac arrhythmias may remain asymptomatic until the first cardiac event, it is relevant to shed light on mutations that could predispose, in association with aging, lifestyle and prior diseases, to the onset of cardiac electrical disturbances. This knowledge will be instrumental not only to enlighten the behavior of the ionic currents, but also in defining new clinical interventions.

The aim of the work is to investigate the impact of T78M cav-3 on the overall cell excitability, focusing also on the role of this variant on the $I_{Kv1.5}$ and I_{HCN4} currents.

MATERIALS AND METHODS

Cell culture and transfection.

Mouse embryonic fibroblasts from caveolin-1 knock-out mice (MEF-KO)(3T3 MEF-KO CRL-2753TM, ATCC) were maintained in DMEM (Life Technologies), supplemented with 10% FBS (Life Technologies) and 1% Penicillin-Streptomycin (Pen-Strep) (Sigma-Aldrich®). All animal procedures were in accordance with the Italian and UE laws (D. Lgs n°2014/26, 2010/63/UE) and approved by the committee of the Università degli Studi di Milano and by the Italian Minister of Health (protocol number 1197/2015). Neonatal rat pups (Sprague Dawley, ENVIGO) were euthanized by cervical dislocation followed by decapitation. Hearts were quickly removed and ventricles were minced in small pieces in PBS and enzymatically digested (from 5 to 8 digestions) by gentle shaking at 37°C in ADS solution (in mmol/L: 116.4 NaCl, 5.4 KCl, 1 $NaH_2PO_4 \cdot H_2O$, 0.8 $MgSO_4 \cdot H_2O$, 5.5 glucose, 20 HEPES, pH 7.4) supplemented with collagenase I (136.8 U/ml, Whorthington) and pancreatine (0.6 mg/ml, Sigma). Neonatal rat ventricular cardiomyocytes (NRVCs) were then maintained in DMEM/M199 (Sigma), added with 10% Horse Serum (Euroclone), 5% FBS (Life Technologies), L-glutamine 2mmol/L and 1% Pen-Strep (Sigma-Aldrich®) at 37°C in a 5% CO_2 incubator. The 233C>T substitution was inserted in the wild type (WT) cav-3 sequence subcloned into the pEGFP-N1 vector using the following primers: forward (5'-cgtctgttgtccatgctgctgggcgt-3'), reverse (5'-acgcccagcagcatggacaacagacgg-3'). In pEGFP-N1 vector, the protein of interest is fused to the eGFP. pCDNA 3.1 plasmids containing the sequence of hKv1.5 (with a V5-flag), hKir2.1 and hHCN4 were used for transfection. For both electrophysiological recordings and sucrose gradient fractionation experiments, MEF-KO cells were plated on 35 mm dishes and co-transfected with 1.5 μg of either the WT or T78M cav-3, or with 0.75 μg of both, and 1 μg of a plasmid containing the ion channel sequence (hHCN4, hKv1.5, hKir2.1) with Fugene HD or ViaFect™ Transfection Reagent (Promega). For electron microscopy experiments, MEF-KO cells were plated on 100 mm dishes and transfected with 13.5 μg/dish of either the WT or T78M cav-3. NRVCs were transfected the day after isolation with either the WT or T78M plasmids (1.5 μg). For membrane staining, MEF-KO cells were co-transfected with also a mix of the pECFP-Mem plasmid (Clontech), that target the protein to lipid rafts, and the pECFP-C1 plasmid(Clontech), that target the proteins to non-rafts membranes.

Immunofluorescence analysis.

48 hours after transfection, immunofluorescence analysis were carried out on living cells transfected with either the WT or T78M cav-3-EGFP and membrane CFP; images were acquired using a laser confocal microscope (Zeiss LSM710).

Electron Microscopy experiments.

For electron microscopy experiments, GFP-positive cells were sorted using flow cytometry (FACS Aria). Two hours after cell sorting, fluorescent cells were fixed as a monolayer in 2% glutaraldehyde in cacodylate buffer 0.1 mol/L (pH 7.4) for 20 minutes at room temperature, scraped and pelleted; cell pellets were further fixed for 24 hours at 4°C. Pellets were post-fixed in 2% osmium tetroxide in cacodylate buffer for 1 hour at room temperature, washed with the buffer, and *en bloc* stained with 1% uranyl acetate in distilled water for 45 minutes. Samples were then dehydrated in increasing ethanol series (70%, 80%, 90%, 100%, and propylene oxide for 10 minutes), and embedded in Epon resin, that was baked at 60°C for 48 hours. Thin sections were obtained with a Leica UC7 ultramicrotome (Leica Microsystems, Vienna, Austria), collected on 300 mesh copper grids, and stained with uranyl acetate and lead citrate. Sections were observed with a Philips CM10 transmission electron microscope (FEI, Eindhoven - Netherlands) at 80 kV. Images were acquired at a final magnification of 25000–92000x using a Morada CCD camera (Olympus, Munster - Germany). All reagents were from Electron Microscopy Science (Hatfield PA).

Separation of membrane fractions.

Transfected MEF-KO cells were lysed in sodium carbonate (pH 11), homogenized with both a loose-fitting tissue homogenizer and a tip sonicator, and then centrifuged. The total protein content of the supernatant was measured with Pierce BCA Protein Assay Kit (Thermo Fisher). 8 mg of total proteins were placed in the bottom of an ultracentrifuge tube in 40% sucrose solution (in 25 mM Mes, 0.15M NaCl, pH 6.5), subsequently covered by discontinuous 35% and 5% sucrose solutions, and centrifuged at 38 000 rpm for 16 hours in a SW40 rotor ultracentrifuge (Beckmann). 12 mL-fractions were collected and divided as follows: fraction 1-3 were discarded; fractions 4-7 were pulled together and represent the cholesterol-enriched fraction (lipid rafts); fractions 8-12 were pulled together and represent the high density fraction (non-lipid raft). Proteins were precipitated for 30 min on ice in 7.92 % trichloroacetic acid. After centrifugation and washing with ethyl ether, pellets were suspended in sample buffer for subsequent western blot analysis.

Co-immunoprecipitation and western blot.

Co-IP buffer used to homogenized MEF-KO cells contained (in mmol/L): 10 Tris, 150 NaCl, 60 octyl-β-D-glucopyranoside, 1% Triton X-100, pH 8 and EDTA-free protease inhibitor cocktail. Samples were centrifuged for 15 min at 10 000 x g at 4°C, and supernatants were immunoprecipitated overnight at 4°C, using 4 µg of the anti-cav-3 antibody (Ab) (Becton Dickinson). As negative controls we either omitted the anti-cav-3 antibody during the immunoprecipitation (IP) or the IP was carried out with the anti-cav-3 Ab on homogenized of MEF-KO cells transfected with channels but not with cav-3 (data not shown). 60 µl of anti-mouse Dynabeads® (Life Technologies) were added and after 2 hours (4°C) the bound protein complexes were eluted in 45 µl of 3X NuPAGE LDS Sample Buffer (Life Technologies) and denaturated at 95°C for 5 min. An aliquot of the clarified lysates used for the immunoprecipitation (input) was run with the eluates on SDS-PAGE with NuPAGE Bis-Tris 4-12% gels (Life Technologies), and revealed by western blotting. For western blotting, anti-cav-3 antibody (1:500), anti-V5 TAG antibody (Sigma-Aldrich; 1:1000) and anti-HCN4 antibodies (Alomone Labs; 1:300) were used. HRP-conjugated and anti-mouse IgG (for anti-cav-3) or anti-rabbit IgG (for anti-HCN4 and anti-V5) secondary antibodies were used. The SuperSignal™ West Femto Maximum Sensitivity Substrate (Life Technologies) was used for the chemioluminescence detection. At the end of the whole procedure, the PVDF membranes were always stained with the amido black staining procedure to assess the efficiency of protein transfer.

Electrophysiology and data analysis.

Cells were superfused with and currents were recorded in Tyrode solution containing (mmol/L): 140 NaCl, 5.4 KCl, 1.8 $CaCl_2$, 1 $MgCl_2$, 5.5 D-glucose, 5 Hepes-NaOH; pH 7.4. To dissect I_{HCN4} current in cardiomyocytes, 1 mmol/L $BaCl_2$ and 2 mmol/L $MnCl_2$ were added to the Tyrode solution. In order to magnify the I_{HCN4}, in MEF-KO cells, the current was recorded using an extracellular solution containing (mmol/L): 110 NaCl, 0.5 $MgCl_2$, 1.8 $CaCl_2$, 5 Hepes-NaOH, 30 KCl, pH 7.4. Patch-clamp pipettes had a resistance of 5-7 MΩ when filled with the intracellular-like solution containing (mmol/L): 130 KCl, 10 NaCl, 5 EGTA-KOH, 0.5 $MgCl_2$, 2 ATP (disodium-salt), 5 creatine phosphate, 0.1 GTP, 10 Hepes-KOH; pH 7.2. In a set of experiments, a saturating concentration of of cAMP (10 µM) was added to the intracellular solution.

hKv1.5 activation curves were obtained from tail currents at -40 mV after activating the current by 200 ms depolarizing steps in the range -60/80 mV applying +10 mV increments.

Inactivation curves were obtained from tail currents at +50 mV after current activation by 10 s depolarizing test steps to the range -60/80 mV. Holding potential (hp) was set at -80 mV. hHCN4 and I_f activation curves were obtained from tail currents at -125 mV preceded by test steps in the range -35/-115 mV in -10 mV steps (hp at -30 mV). Activation and inactivation curves were fitted with the Boltzmann equation:

$$y=1/(1+\exp((V-V_{1/2})/s))$$

where V is voltage, y the fractional activation, $V_{1/2}$ the half-activation voltage or the half-inactivation voltage, and s the inverse-slope factor. hHCN4 activation time constants were obtained by fitting the current traces obtained from the activation protocol using a mono-exponential function. Deactivation time constants were similarly obtained by fitting deactivating current traces recorded in the range -65/+25 mV after a fully activating voltage step at -125 mV.

For current density analysis, current intensity at each potential was normalized by cell capacitance. hKir2.1 current was analyzed as the Ba^{2+}-sensitive component elicited by 10 mV voltage steps in the range -100/10 mV (hp -80 mV). Spontaneous action potentials were recorded from small aggregates of fluorescent cells (2-4 cells/aggregate). Inter-beat interval (IBI) is defined as the time from one action potential peak to the next one. The coefficient of variation of IBI (CV_{IBI}) was defined as the ratio between σ_{IBI} and $\overline{IBI}$. NRVCs were measured at 37±1°C.

Genetic analysis.

The investigation conforms to the principles outlined in the Declaration of Helsinki. For caveolin-3 gene screening, approval was granted by ethic review board of the University of Milan. Written informed consent was obtained from the patients or parents prior to carrying out genetic analysis on genomic DNA extracted from whole blood or saliva (Puragene Blood Kit, Qiagen). The coding sequence of CAV3 was amplified by PCR using the following primers: for exon1, 5'ccaagtattttcagccccag3' (F) and 5'cctcggcgggcggagagtgt3' (R); for exon2 5'gggtggcttctgtgagttga3' (F) and 5'agaaagaaaagacggcccag (R). The PCR reaction mixture included 100 ng of genomic DNA, 1 μmol/L primers and the FastStart Taq DNA Polymerase (Roche). Analysis of the amplicons was carried out by DNA sequencing (Bio-Fab Research).

Computational analysis.

On the original Grandi-Bers model[38] of human atrial cell, we introduced the I_f current formulation from the Koivumaki model[39]:

$$I_f = I_{fNa} + I_{fK}$$

$$I_{fNa} = 0.2677 \cdot g_f \cdot Xf \cdot (V - E_{Na})$$

$$I_{fK} = (1 - 0.2677) \cdot g_f \cdot Xf \cdot (V - E_K)$$

$$g_f = 1 \quad \text{nS}$$

$$\frac{dXf}{dtime} = \frac{xf_{inf} - Xf}{\tau_f}$$

$$xf_{inf} = \frac{1}{1 + e^{\frac{V+86.2}{9.66316}}}$$

$$\tau_f = \frac{1}{0.00332 \cdot e^{-\frac{V}{16.54103}} + 23.71839 \cdot e^{\frac{V}{16.54103}}}$$

The I_{Na} late current was added as previously[38]

$$I_{Na\_late} = g_{Na\_late} \cdot m^3 \cdot h \cdot (V - E_{Na})$$

$$\frac{\mathrm{d}m}{\mathrm{d}time} = \alpha_m \cdot (1 - m) - \beta_m \cdot m$$

$$\alpha_m = 0.32 \cdot \frac{V + 47.13}{1 - e^{\frac{-47.13-V}{10}}}$$

$$\beta_m = 0.08 \cdot e^{\frac{-V}{11}}$$

$$\frac{\mathrm{d}h}{\mathrm{d}time} = \frac{h_{inf} - h}{\tau_h}$$

$$h_{inf} = \frac{1}{1 + e^{\frac{V+91}{6.1}}}$$

$$\tau_h = 600 \quad \text{ms}$$

with a maximal conductance of 0.8575 S/F. In this way, under voltage clamp simulation, a late component was introduced (0,11% of the peak current, as reported by Cronk and colleagues[31]). The intracellular potassium concentration was set to 140 mmol/L and the maximal conductance of the I_{K1} current was slightly increased (8%) in order to restore the original resting potential. The T78M condition was implemented after the insertion of the effects on the If and IKur current recorded in our experiments in MEF-KO cells and by setting

the late INa conductance to 4.0216 S/F (equal to 0.48% of the peak current, as reported by Cronk et al.[31]). The model was paced at 1 Hz until steady state was reached. Since computational model of human sinoatrial cell are still not available, we used the Sever-DiFrancesco model of single sinoatrial node cell. The steady-state I_{Na} inactivation slope was slightly increased in order to reproduce, under voltage clamp in control conditions, an amount of late INa current equal to 0.11% of the peak current. To model the T78M condition, the late INa current was added with a maximal conductance of 0.5306 nS (equal to 0.48% of the peak current). Effects on If were also implemented as reported above. All numerical simulations and data analysis were performed in Matlab (Mathworks, Inc.).

Statistical analysis.

Data were compared with nested ANOVA using SPSS Statistics (IBM), setting the type of cav-3 (WT, T78M, WT/T78M) as fixed factor and the transfection as nested factor. Since transfection did not result in a significant factor on any parameter analyzed, data were subsequently compared considering only the type of cav-3 as categorical factor, hence using one-way ANOVA followed by Fisher's post hoc test. Activation and inactivation curves were evaluated by comparing the mean $V_{1/2}$ values derived by the Boltzmann fitting using one-way ANOVA followed by Fisher's test. Significance level was set to p=0.05.

RESULTS

The T78M cav-3 reaches the membrane and does not alter the formation of caveolae.

To address the cellular localization of the T78M cav-3 variant, we took advantage of cav-3 proteins fused with eGFP fluorescent proteins. Figure 1 shows live staining of MEF-KO cells transfected with either the WT or the T78M cav-3. In addition, we co-transfected fluorescent plasmids able to stain the plasma membrane (pm) (see Material and Methods). As clearly visible, both the WT (Fig.1, top) and the T78M cav-3 (Fig.1, bottom) reaches the membranes (yellow signal).

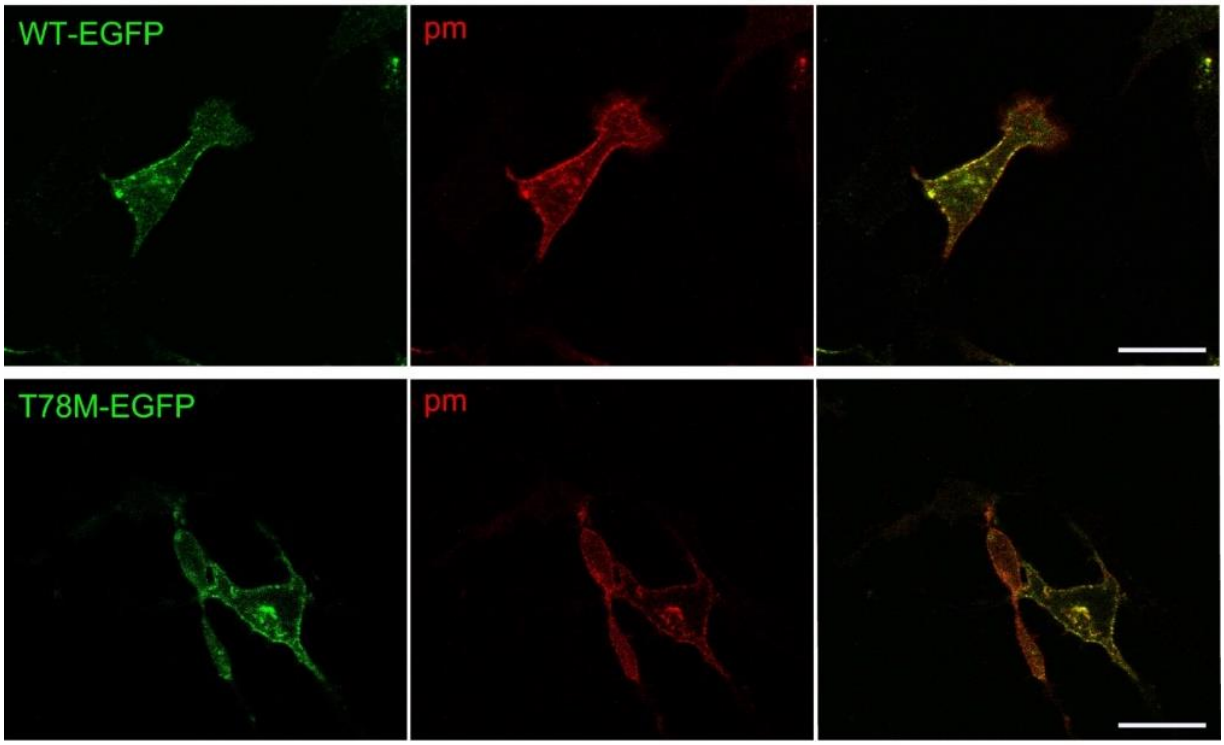

Figure. 1. T78M cav-3 is localized in the plasma membrane. Representative live staining confocal images of MEF-KO cells transfected with either the WT (green, top) or T78M (green, bottom) cav-3. All cells were also co-transfected with membrane-targeted CFP plasmid (pm, red, center). Right panels shows signals overlapping(yellow). Exp=3; scale bar=20μM.

Despite this result showed the correct plasma membrane localization of the cav-3 variant, it was not informative about the proper generation of the caveolar structure. We thus performed electron microscopy experiments in order to evaluate the ability of cells expressing the T78M variant to proper generate the caveolar structure. We firstly assessed that our cellular system completely lacks caveolae as well as caveolins (Fig.2A). We found that in MEF-KO cells transfected with either the WT or T78M cav-3 (Fig.2B and 2C, respectively), the caveolae (arrows) were properly detected at the plasma membrane. In particular, we found an equal

amount of caveolar structure per unit of length in the presence of either the WT or T78M cav-3, as summarized in the bar graph in Fig.2D. These results suggest that the T78M cav-3 is able to reach the membrane without affecting neither caveolae formation nor distribution.

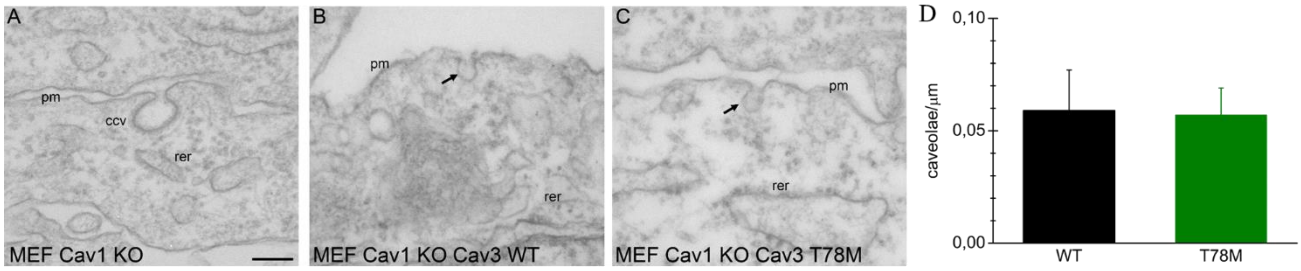

Figure. 2. Caveolae formation and distribution is not affected by T78M cav-3. A-C) Representative transmission electron micrograph section in non-transfected MEF-KO and MEF-KO transfected with either the WT or T78M cav-3 (from left to right, respectively). Arrows indicate caveolae structure at the plasma membrane (pm). **D)** Bar graph of the mean caveolae distribution in WT (black) or T78M (green) transfected MEF-KO cells (WT: 0.056± 0.007 cav/mm n= 25, T78M:0.053± 0.006 cav/mm; n=25, from 3 experiments). rer, rough endoplasmic reticulum; N, nucleus; G, Golgi apparatus; M ,mitochondrion. Scale bar =150 nm.

The T78M cav-3 is present in the low-density fractions and binds both hKv1.5 and hHCN4.

We analyzed if the T78M cav-3 is present in the lipid rafts fraction (LR), as previously reported for the WT isoform. Moreover, we also checked if hKv1.5 and hHCN4 still resides in the lipid rafts fraction. We chose these channels not only because they were shown to bind to cav-3[18,25], but their dysfunction has already been associated with arrhythmias[40,41]. We firstly found that, after the separation of the membrane fractions based on their density using a discontinuous sucrose gradient, both the WT and the T78M cav-3, together with both ion channels, are present in the LR phase, as visible in the representative blots showed in Figure 3A. We subsequently checked if both hHCN4 and hKv1.5 were bound by the T78M cav-3. The representative blots showed in Figure 3B from co-immunoprecipitation experiments demonstrated that, similarly to the WT isoform, the T78M cav-3 is able to bind both channels. These results demonstrated that the point mutation did not affect neither the binding with both hKv1.5 and hHCN4 channels nor their localization in the LR phase.

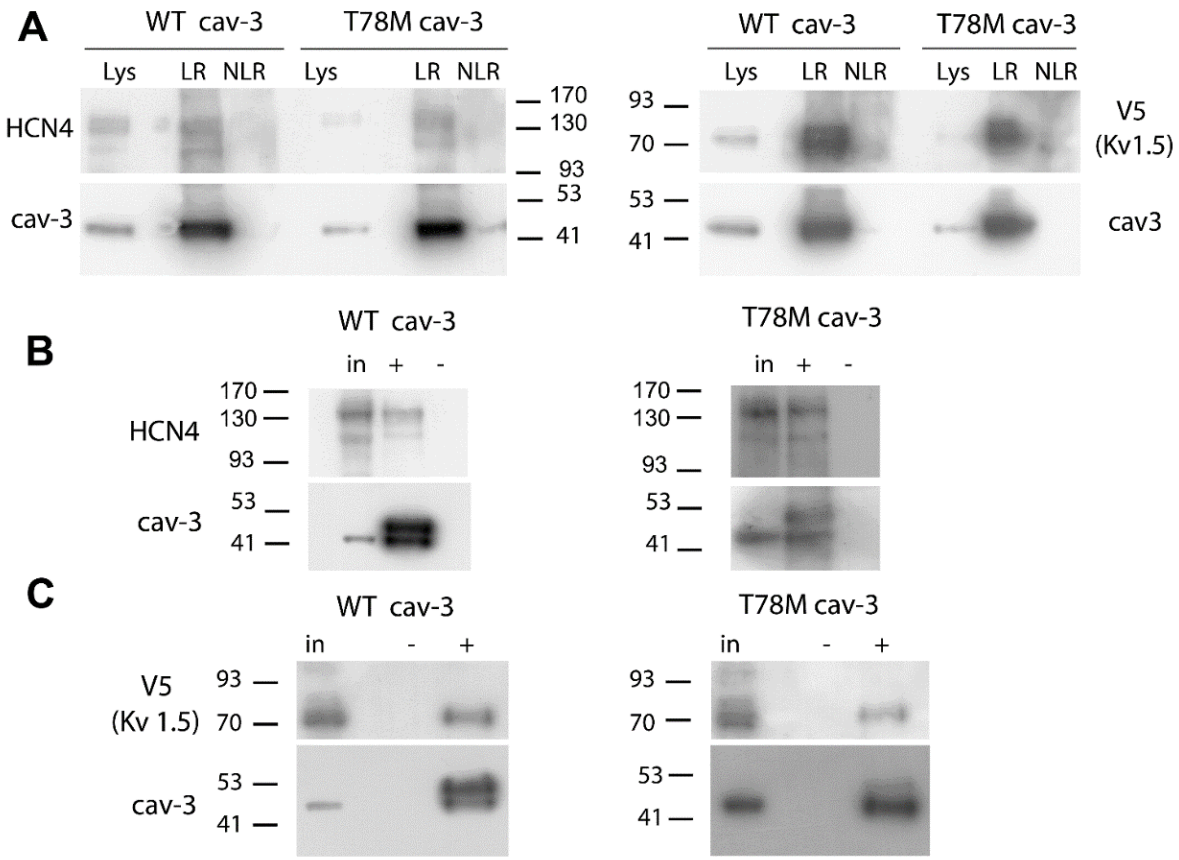

Figure. 3. T78M cav-3 interacts with both hHCN4 and hKv1.5 and targets them to the lipid raft domain. A) Representative blots of hHCN4 (left) and hKv1.5 (right) expressed in MEF-KO transfected with either the WT or T78M cav-3 isolated by discontinuous sucrose gradient (n>2; Lys, lysate; LR lipid raft fractions; NLR non-lipid raft fractions). **B,C)** Co-immunoprecipitation (co-IP) experiments from MEF-KO cells co-transfected with either HCN4 (B) or V5-Kv1.5 (C) and WT cav-3 EGFP or T78M cav-3 EGFP (n= 3). An aliquot of the input (in) and of the co-IP eluate (+) were tested by western blot. A negative control (–) was performed by omitting the cav-3 antibody in the IP procedure.

The T78M cav-3 alters the kinetic properties of hKv1.5 without affecting current density.

After the assessment of the binding between T78M cav-3 and hKv1.5, we analyzed its impact on the electric properties of the potassium channel. Thus, we transfected MEF-KO cells with either the WT, T78M or both cav-3 isoforms with the hKv1.5, as indicated in the Figure 4.

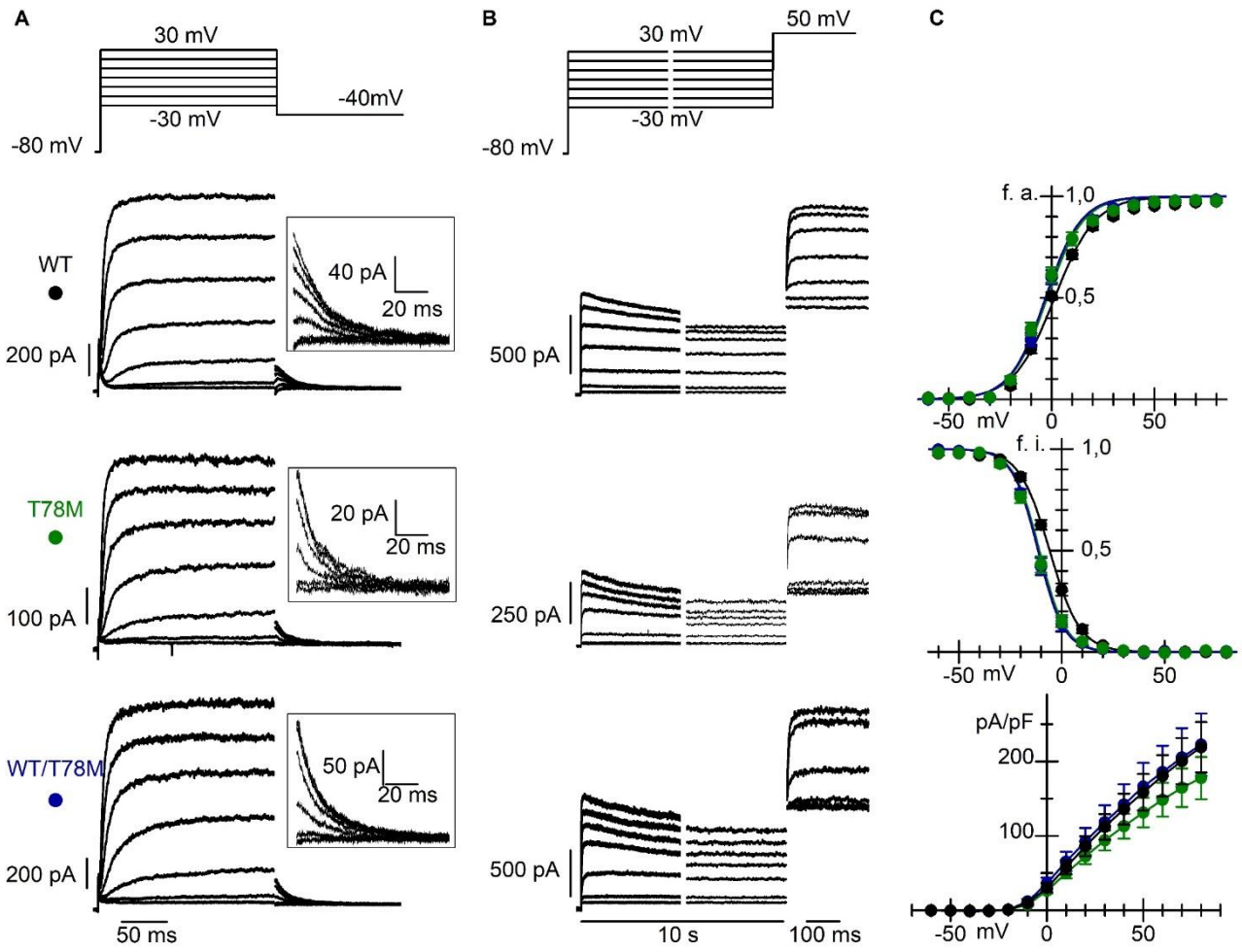

Figure. 4. T78M cav-3 affects kinetic properties of $I_{Kv1.5}$. A) Representative traces of $I_{Kv1.5}$ current elicited applying the activation protocol (top) in MEF-KO cells transfected with the WT, T78M or both cav-3 as indicated. The insets represent a magnification of the tail currents. **B)** Representative $I_{Kv1.5}$ traces obtained in response to the inactivation protocol (top) in the different conditions as indicated. **C)** Bar graphs of the mean activation (top; $V_{1/2}$ values (mV): WT 1.41± 0.70, n=27; T78M –2.63± 1.43*, n=23; WT/T78M –2.21± 1.15*, n=17), inactivation (center; $V_{1/2}$ values (mV): WT –5.9± 0.9, n=24; T78M – 10.9± 0.9*, n=24; WT/T78M – 11.5± 0.6*, n=18) and current density-voltage relation (bottom; WT n= 22, T78M n=26, WT/T78M n= 21). (f.a., fraction of activation; f.i., fraction of inactivation; WT, black; T78M, green; WT/T78M, blue). *p<0.05 by nested and One-way ANOVA with Fisher's test compared to WT cav-3.

Representative traces of $I_{Kv1.5}$ current elicited in response to the activation (Fig. 4A) or inactivation (Fig. 4B) protocol are shown in the WT, T78M or WT/T78M transfected cells (top, center and bottom, respectively). As summarized in the mean activation (top) and inactivation (center) curves in Figure 4C, we found a significant leftward shift of both in the presence of the T78M cav-3. Importantly, the T78M cav-3 behave as a dominant variant, since the co-expression with the WT isoform is functionally indistinguishable compared to homozygous T78M cav-3. In particular, we found -4.04 and -3.62 mV shifts in the mean activation curves in T78M and WT/T78M cav-3 compared to WT cav-3 cells, respectively.

Furthermore, the mean inactivation curves of T78M and WT/T78M cav-3 cells compared to the WT ones were shifted by -5.00 and -5.60 mV, respectively. In opposition, the current density was not affected (Fig.4 C, bottom). These results suggest that T78M exclusively affects the kinetics of the channel inducing a gain-of-function of the $I_{Kv1.5}$ current.

The T78M cav-3 induces a rightward shift of the activation of hHCN4 channels.

We also analyzed the impact of the variant on the biophysical properties of the current conducted through the hHCN4 channels. In Figure 5A, superimposed normalized traces of I_{HCN4} elicited at -85 mV and followed by a fully activating step at -125 mV are shown. A significant rightward shift of the mean activation curves is shown in Figure 5B in the presence of the T78M cav-3 in a dominant negative way (+7.90 and +8.80 mV of shift for the T78M and WT/T78M cav-3, respectively).

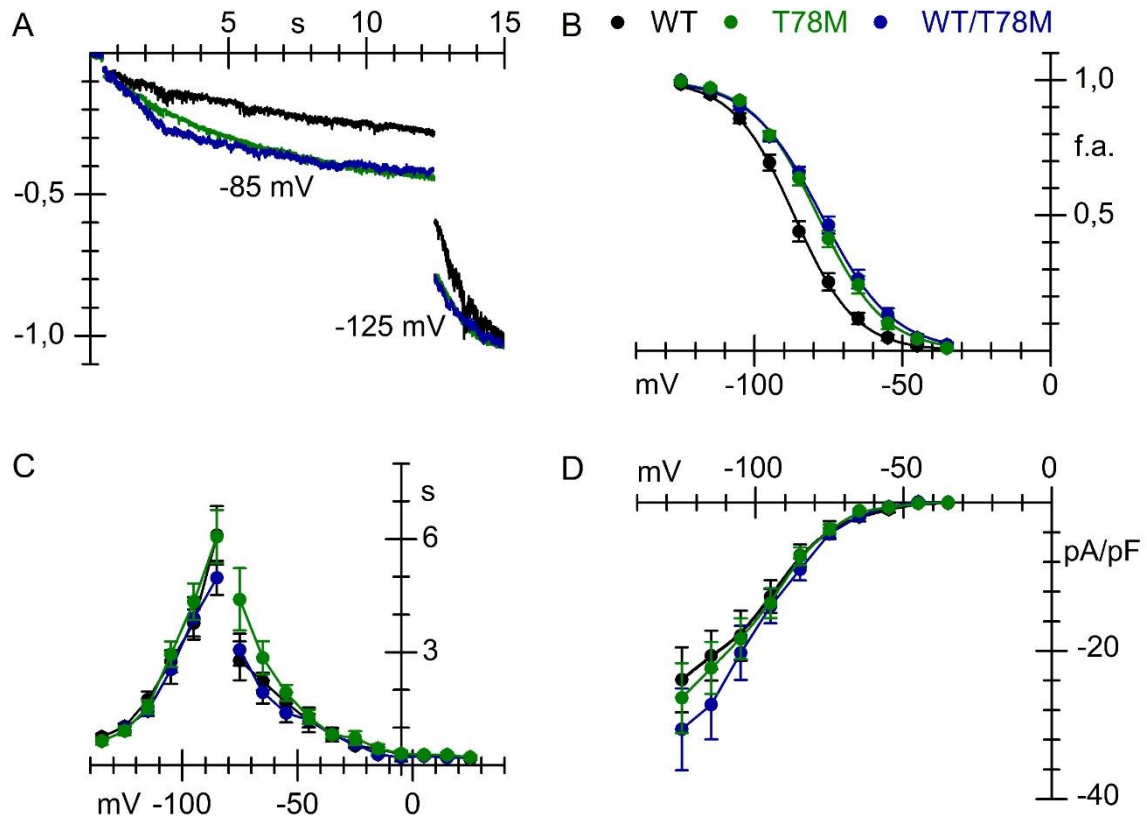

Figure. 5. The T78M cav-3 affects the open probability of hHCN4 channels. A) Representative traces of I_{HCN4} currents, normalized and overlapped, were elicited in response to a double-protocol step (-85/-125 mV) from a holding potential of -30 mV. Current traces were shown for MEF-KO cells overexpressing the WT (black), T78M (green) and WT/T78M (blue) cav-3. **B)** Mean activation curves ($V_{1/2}$ values in mV: WT –86.2± 1.1, n=26; T78M –78.3± 1.1*, n=30; WT/T78M –77.4± 1.0*, n=29), **C)** mean τ values (WT, n=20; T78M, n=14; WT/T78M, n=20) and **D)** mean current density-voltage plot (WT, n=20; T78M, n=14; WT/T78M, n=20). (f.a., fraction of activation) *p<0,05 by nested and One-way ANOVA with Fisher's test compared to WT cav-3.

We did not find modifications of both the kinetics of activation and deactivation (Fig. 5C). Similarly, we did not found any modification of the I_{HCN4} current density (Fig. 5D). Since the T78M cav-3 induced a rightward shift of the activation curves for hHCN4, and considering that a rightward shift could be induced after the binding of cAMP to the HCN channels, we asked if the shift could be addressed by cAMP.

	Untreated		**cAMP (10 µM)**	
Cav3	**$V_{1/2}$ (mV)**	**s (mV)**	**$V_{1/2}$ (mV)**	**s (mV)**
WT	-85,3 ± 1,1 (n=5)	9,7 ± 0,2 (n=5)	-73,4 ± 1,5§ (n=11)	10,3 ± 0,4 (n=11)
T78M	-77,9 ± 1,2* (n=6)	10,3 ± 0,6 (n=6)	-71,9 ± 1,0§ (n=16)	10,8 ± 0,4 (n=16)
WT/T78M	-77,8 ± 1,5* (n=8)	10,0 ± 0,4 (n=8)	-72,5 ± 1,5§ (n=8)	9,9 ± 0,6 (n=8)

Table 1. $V_{1/2}$ and inverse slope factor (s) values in MEF-KO transfected with either WT, T78M or both with or without saturating concentration of cAMP. *p <0.05 by nested and One-way ANOVA with Fisher's test compared to WT cav-3. §p<0.05 by Student's T-test compared untreated condition.

After testing saturating concentration of cAMP in the pipette (10 µM), we found that the rightward shift was present in WT as well as T78M transfected cells (p<0.05). However, it is important to notice that the difference after and before cAMP treatment was higher in WT compared to T78M cells. These results indicate that T78M cav-3 induces a gain-of-function of the current modifying only the kinetic parameters.

Overall membrane excitability is affected in the presence of the T78M cav-3.

In order to test the effect of the T78M cav-3 on the overall membrane excitability behind the characterization of the single ionic currents, and taking advantage of the dominant negative effect of the variant, we also decided to analyze the impact of the T78M cav-3 in the neonatal rat ventricular cardiomyocytes (NRVCs). This cellular system express not only the cav-1 and cav-3 isoforms, but it also possess most importantly the ionic currents that sustained the spontaneous action potential firing.

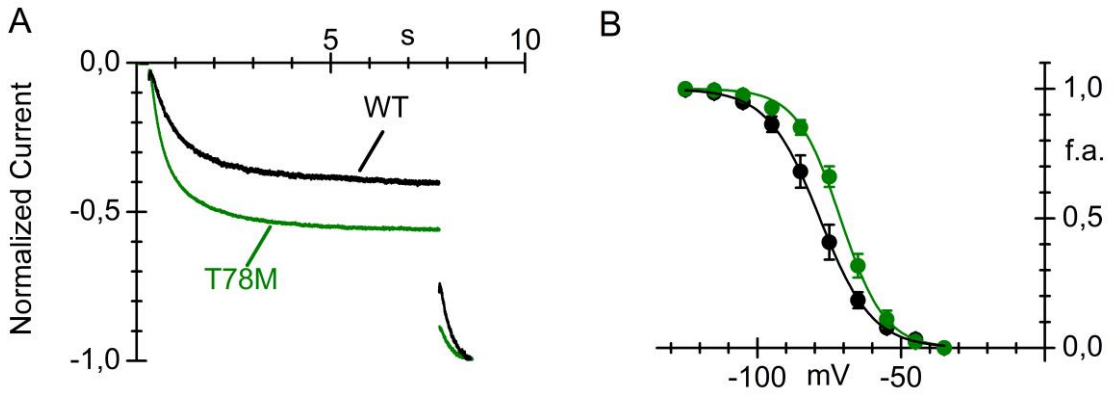

Figure. 6. Funny current is affected by the T78M cav-3 in cardiomyocytes. A) Normalized and overlapped current traces of funny current elicited by -85/-125 mV from a holding potential of -30 mV. **B)** Mean activation curves ($V_{1/2}$ values in mV: WT –77.51± 1.9, n=9; T78M –70.57± 1.0*, n=9). (f.a., fraction of activation; WT, black; T78M, green). *p<0.05 by Student's t-test.

We firstly tested the effect of T78M on I_f native current. In Figure 6, the mean activation curves of WT *vs* T78M cav-3 cells showed a significant rightward shift of T78M cav-3 cells, similarly to the previous one found in the MEF-KO cells. In Figure 7A, time courses of the inter-beat interval (IBI) are shown. It is clear that a more stable action potential firing was present in both empty vector (EV) and WT cav-3-transfected cells compared to T78M cav-3 cells (top, middle and bottom, respectively), as also visible from the representative stretches of action potential showed in the insets.

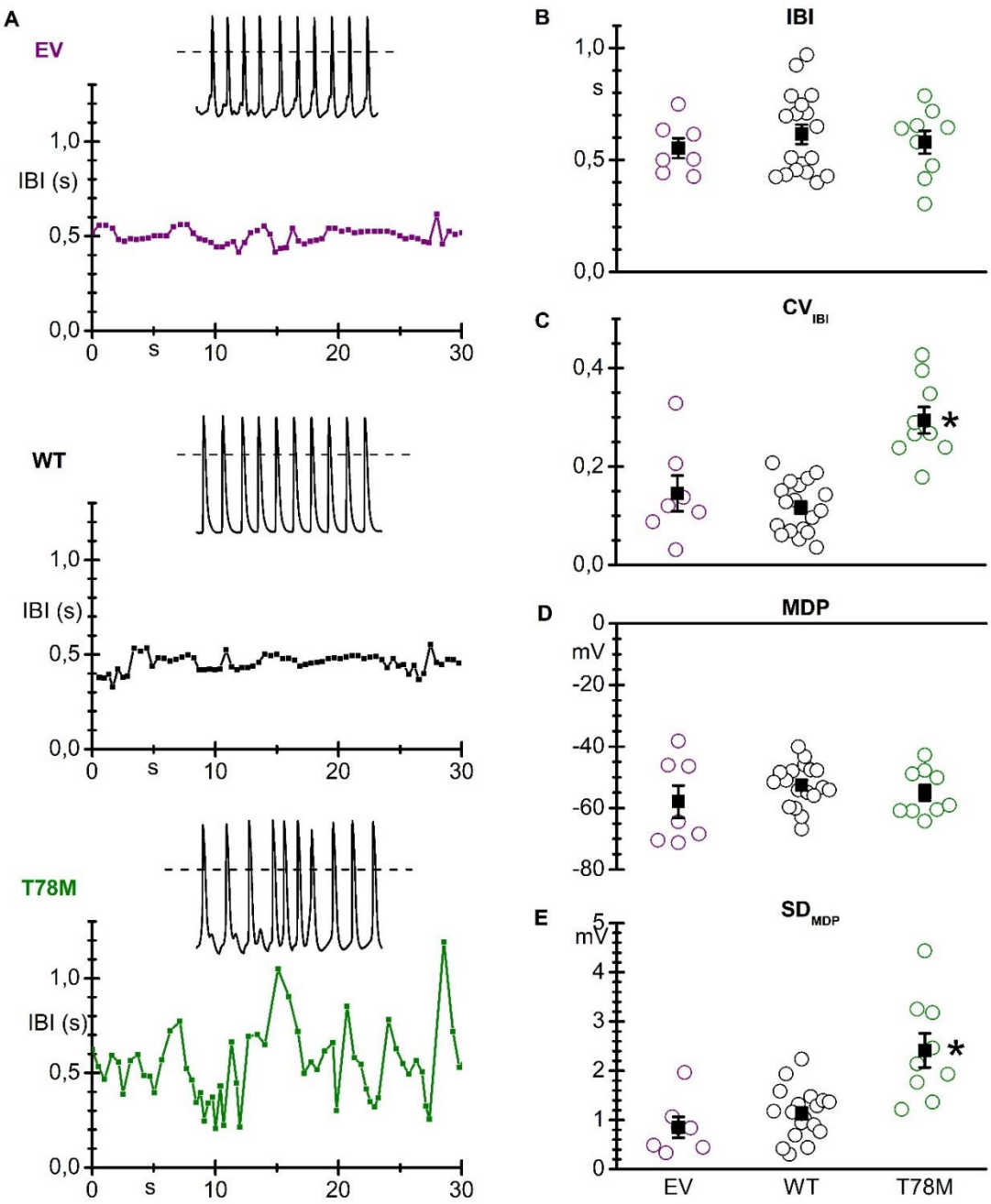

Figure. 7. The generation of action potential is compromised in myocytes expressing T78M cav-3. A) Time courses of the inter-beat interval (IBI) in neonatal rat ventricular cardiomyocytes (NRVCs) transfected with the empty vector (EV, purple), the WT (black) and the T78M (green) cav-3. The insets show 5 seconds representative stretches of action potential recorded in the different conditions. Scatter plot showing the single values of **B)** the IBI values (in s: EV 0.55± 0.04, n=7; WT 0.61± 0.04, n=18; T78M 0.58± 0.05, n= 9), **C)** the coefficient of variation of IBI (CV_{IBI}; EV 0.14± 0.04; WT 0.12± 0.01; T78M 0.29*± 0.03), **D)** the maximum diastolic potential (MDP; in mV: EV –57.9± 5.2; WT –52.6± 1.6; T78M –55.1± 2.5) and **E)** the standard deviation of MDP (SD_{MDP}; in mV: EV 0.85± 0.21; WT 1.13± 0.12; T78M 2.41*± 0.35). *p< 0.05 vs. all other conditions by nested and one-way ANOVA with Fisher's test.

The mean IBIs were summarized in the Figure 7B, and no significant differences were detected among the analyzed condition. However, the coefficient of variation of the IBI

(CV_{IBI}) is significant higher in the T78M cav-3 NRVCs, as summarized in Figure 7C. We also evaluated the maximum diastolic potential (MDP) and, again, we found no significant differences in the mean values of this parameter in the three conditions (Fig. 7D), whereas its variability is significantly affected in the T78M expressing myocytes (Fig. 7E). These results showed that the T78M cav-3 is able to influence the overall stability of the action potential firing.

The T78M cav-3 is found with a high frequency in patients affected by supraventricular arrhythmic diseases.

Since these *in vitro* results pointed out that T78M cav-3 could induce a pro-arrhythmic substrate, we analyzed the frequency of this variant in a cohort of healthy controls, arrhythmic patients and stillbirths (these last were negative for mutations in *KCNQ1*, *KCNH2* and *SCN5A* genes). In Table 2, the specific composition of the cohorts is enlisted as well as the number of allele carrying the T78M variant. We found a significant higher MAF in patients with atrial fibrillation, IST and stillbirths compared to bradycardic patients and healthy controls.

Pathology	Allele count/ number	Allele frequency
Inappropriate Sinus Tachycardia (IST)	4/92*	4.35%
Atrial Fibrillation (AF)	2/32*	6.25%
Stillbirth	2/74*	2.7%
Sinus Bradycardia	1/222	0.45%
Unaffected controls	0/418	0%
General population (ExAC)	367/120800	0.3%

Table 1 Frequencies of the 223C>T substitution

This data indicates that T78M cav-3 is a predisposing factor in supraventricular arrhythmic disorders, even if larger epidemiological studies are necessary.

***In silico* analysis of atrial and sinoatrial single cell showed a pro-arrhythmogenic action potential profile.**

The above-mentioned *in vitro* experiments were performed using an overexpression approach on heterologous and immature cells; thus, we also tested the effect on the overall membrane excitability of the T78M cav-3 using an *in silico* approach. In particular, we modeled the T78M-induced modification of ionic currents in two adult cellular system, single atrial cell and rabbit sinoatrial node cell, since we found this variant in a population affected by supraventricular arrhythmias (Tab. 2). In single atrial cell, we inserted the modification

related to the I_f and I_{Kur} current as well as the previously reported modification on both late I_{Na} and I_{K1} currents. Accordingly to the numerical reconstruction shown in Figure 8A, the insertion of the reduction of about 75% of I_{K1} generated an action potential unable to correctly repolarize to its resting potential, and thus incompatible with life. For this reason, we checked in the MEF-KO system the effect of the T78M cav-3 on I_{K1} current funding no significant reduction of the current density, as summarized in the plot in Figure 8B.

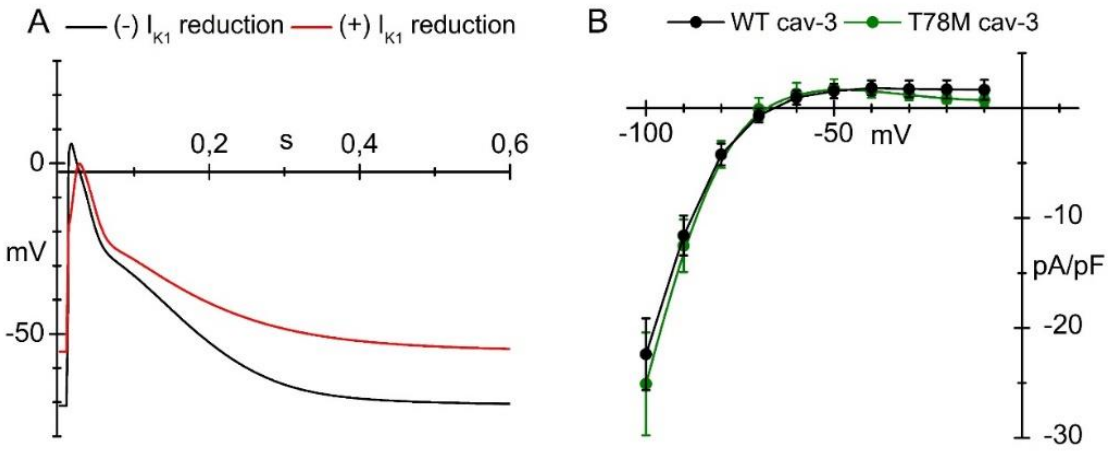

Figure. 8. The T78M cav-3 did not alter the IK1 current density. A) Atrial action potential generated using the Grandi-Bers human atrial cell model. **B)** I_{K1} current density voltage plot recorded as the Ba^{2+}-sensitive current in MEF-KO cells.

We subsequently modeled the above-mentioned modification but omitting modification of I_{K1}. The result is shown in Figure 9A, in which a clear shortening of the Action Potential Duration (APD) at the 50% or 90% (APD50 and APD90) appeared as well as a mild depolarization of the resting potential and a reduction of the peak potential.

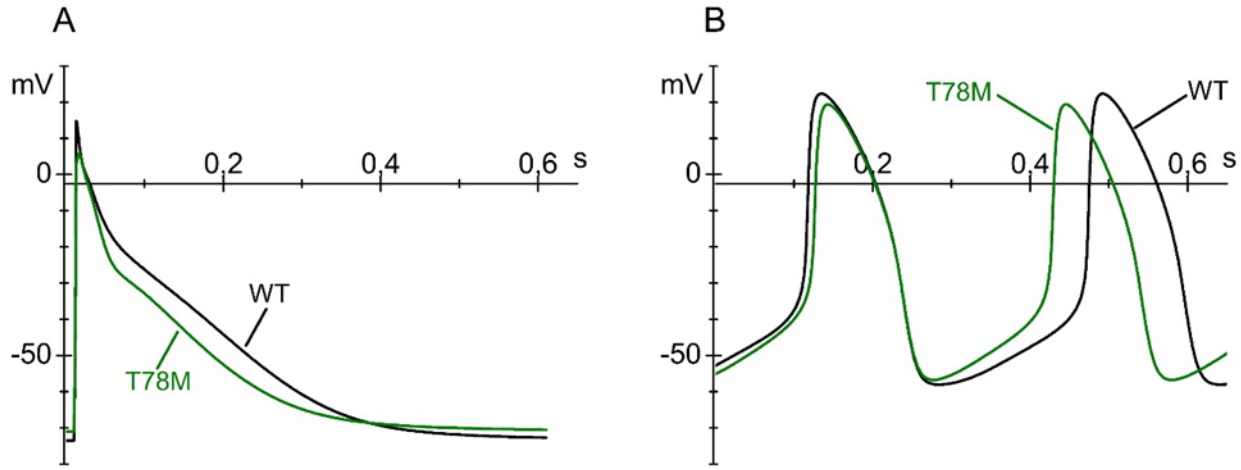

Figure. 9. Mathematical models of both atrial and sinoatrial cells show an arrhythmogenic profile in the presence of the T78M cav-3. Action potential generating using **A)** the Grandi-Bers model of human atrial cell

and **B)** the Severi-DiFrancesco model of rabbit sinoatrial cell. In black the basal condition (WT); in green, after the insertion of T78M-dependent alterations.

The simulation was also carried out using a model of rabbit single sinoatrial cell in which the modification of both I_f and I_{Na} late was inserted. The resulting simulation is shown in Figure 9B. We found an increase of the diastolic depolarization rate that led to an increase in firing rate. Mild modification of the other parameters were found (APD90 –6%, Maximum Diastolic Potential +1mV, upstroke potential –3mV).

Taken together, these results reinforce the idea that T78M cav-3, at least at the cellular level, is able to induce pro-arrhythmic modifications altering the biophysical properties of the ionic currents restricted in the caveolar domain.

DISCUSSION

Arrhythmias, Part 1: in search of ion channel mutation.

The term arrhythmias refers to any modification from the normal sequence of electrical impulses in the heart. This is a life-threatening condition that affects an increasing fraction of the population. Accordingly to the American Heart Association guidelines, an arrhythmia occurs when: 1) the natural pacemaker of the heart, the sinoatrial node (SAN), develops an abnormal rate; 2) another region takes over as pacemaker and 3) the spatiotemporal conduction is erratic. Despite the clinical manifestations and etiology of arrhythmias are extremely heterogeneous and complex, all these electrical disturbances share a common point: the ion channel activity of cardiomyocyte is impaired. Over the past 20 years, geneticists, molecular cardiologists, and electrophysiologists have collected a wealth of information regarding ion channels[42]. They found that the phenotype of some patients could be explained by the expression of mutated ion channels. The first case was reported by Mark Keating in the 1998[43]; it was the first evidence of the link between *SCN5A* mutations and the LQTS, *de facto* funding the discipline of cardiac channelopathies. Indeed, scientists defined cardiac channelopathies any arrhythmic disorders of genetic origin related to improper ionic control of the cardiac action potential. This work clearly showed that a single point substitution carried by ion channels is able to produce significant modification in the electrophysiology of the cell. The paradigm "genetic arrhythmias-ion channel mutations" allowed the identification of a plethora of rare mutations clearly associated with several arrhythmic syndromes[44]. These advancements had transformed the clinical approach to the diagnosis and treatments of such conditions. However, a new paradigm must be taken in consideration.

Arrhythmias, Part 2: beyond ion channel mutation.

Beyond the biophysical characteristics of the ion channels, the cellular microenvironment affect the ionic currents as well. Among protein interacting with ion channels, caveolin-3 (cav-3) is a key player in the formation of caveolae in muscle cells. Caveolae are membrane domains with peculiar lipoprotein composition that influence, among other things, signal transduction processes[6]. The integrity of the caveolar domain has been associated with the correct function of the residing ion channels[19,23]. Mutations on *CAV3* define the family of diseases known as caveolinopathies[26]. The main pathologies associated with *CAV3* mutations are limb girdle muscular dystrophy 1-C (LGMD), HyperCKemia (HCK), rippling muscle disease (RMD), distal myopathy (DM), familial hypertrophic myopathy (FHM), Long-QT

syndrome (LQTS) and some cases of sudden infant death syndrome (SIDS)[28]. In literature, the association between cav-3 defects and skeletal muscle disorders are well documented[45]; on contrary, the role of cav-3 variants in a cardiac context is weaker due to the lacking of data from a cardiologic point of view. It is important to notice that the caveolinopathies could be better define as a continuous spectrum of pathologies since the same mutation could be identified in patients affected by different syndromes. This behaviour suggest that the *CAV3* mutation are not causative of the phenotype, but that they could participate in the onset of a broad range of pathologies in association with the peculiar genetic and environmental background of the patient. The interpretation of the molecular basis for cardiac arrhythmia susceptibility is a hot topic in both basic science and clinical management of arrhythmic syndromes. The most controversial *CAV3* mutation is the T78M.

Who: the T78M cav-3. A variant or a mutation?

The T78M cav-3 was previously found in patient affected by RMD, proximal myopathy, LQTS, idiopathic hyperCKemia, and SIDS[28,30-32]. We identify the T78M cav-3 in patients affected by inappropriate sinus tachycardia, atrial fibrillation and in case of stillbirth (Tab.2). In our small cohort of healthy controls, we never identified the variant. On the contrary, Spadafora *et al.*[37]reported the T78M cav-3 as a common polymorphism in South Italy. Moreover, we did not screened patients affected by LQTS and SIDS since was previously reported that the frequency of the T78M cav-3 was similar to that found in healthy controls and in the exome sequencing project[35,36]. These works argued against a causative effect of the T78M in the etiology of the pathologies. However, it is important to mention that, for cardiac arrhythmias, it is hard to define the healthy control group since, in many cases, the patients were asymptomatic until the first event. Despite larger epidemiological analysis will be required and the fact that the T78M cav-3 exhibits incomplete penetrance, variable expressivity, and phenotypic overlap, our data enlarge the clinical spectrum of diseases associated with the T78M cav-3. The absence of a clear genotype-phenotype association suggest that the T78M cav-3 is a genetic predisposing factor necessary, but not sufficient, to induce the phenotypic spectrum of disorders. Strategies to properly interpret the influence of mutations that have divergent effects are required; as stated by Schwartz *et al*: "The lack of functional or biological validation of mutation effects remains the most severe limitation of genetic test interpretation in the cardiac channelopathies"[44]. In such genotyping chaos, we need to reconsider the importance of phenotype-guided genetic testing[46]. We thus decide to deepen the molecular characterization of the T78M cav-3, in particular on the functional effect of the variant on membrane excitability.

Where: the cellular localization of the T78M cav-3.

The first relevant issue was to check the localization of the T78M cav-3. In literature, the localization of the variant seems to be cellular-dependent [32,33]. We used a cellular system derived from mice lacking the *CAV1* gene, the mouse embryonic fibroblast (MEF-KO) cells. The clear advantage of this system is the absence of caveolar structures (Fig. 2A), since the expression of the cav-3 isoform is restricted to muscular cells. Both the WT and T78M cav-3 properly reach the plasma membrane (Fig.1). Moreover, the T78M cav-3 still resides in the lipid raft domain (Fig.3A). We also found that both hKv1.5 and hHCN4 are able to binding the T78M cav-3 and hence reside in the lipid raft domain (Fig. 3B). We analyzed these two ion channels since they have been associated with supraventricular arrhythmic disorders[47,48] and were influenced by the proper maintenance of the caveolae integrity, as previously demonstrated[19,23]. However, the plasma membrane localization of the T78M cav-3 did not automatically implied the correct generation of the caveolar structure, nor their distribution. To address this, we performed electron microscopy experiment that confirm the presence of caveolae also in MEF-KO cells transfected with the T78M cav-3 (Fig. 2). Despite more insight on the composition and functional integrity of caveolae will be mandatory, it seems that the T78M cav-3 does not affect the process of generation of the caveolar domain.

What and how: the effect of the mutation on the ion channel activity and membrane excitability.

We asked if, in spite of proper membrane localization of the variant and apparent integrity of the caveolar domain, the T78M cav-3 could alter membrane excitability. We started analyzing the effect of the T78M cav-3 on the properties of I_{Kur}. We found that, in agreement with the Co-IP experiments, the T78M cav-3 did not alter the I_{Kur} current density (Fig. 4C). On the other hand, the variant affects the kinetic properties of the channel in a dominant negative way (Fig. 4C). In particular, T78M cav-3 induces a significant leftward shift of both activation and inactivation curves. These modifications result in a gain-of-function of the I_{Kur} current, hence a major contribution to the repolarizing phase of the atrial action potential. In fact, even if the leftward shift of the inactivation curve indicates lower channel availabilityof, and thus a loss-of-function effect, the inactivation process for $K_v1.5$ channels is an order of magnitude slower than the activation one. A gain-of-function behaviour of the I_{Kur} was previously associated with arrhythmic disorders and it is compatible with the atrial fibrillation phenotype[41]. Similarly, modifications of the kinetic properties were also found after the

chemical depletion of cholesterol from the membrane[19]. The presence of the channels in the lipid rafts domains, however, lead us to exclude the shift of the channel from caveolar to non caveolar domains in the presence of the T78M variant.

The T78M variant is also able to induce a rightward shift of the mean activation curve of HCN4 channels (in MEF-KO; Fig. 5) and of the funny channels (in NRVCs; Fig. 6). This imply that, at the same voltage, a higher amount of current flows through the HCN channels; hence, the T78M cav-3 induces a gain-of-function of this current. Again, the effect is exerted in a dominant negative way. This modification is compatible with the inappropriate sinus tachycardia[40], a phenotype in which we identified the variant. Moreover, a gain-of function of the I_f current has been previously associated with atrial fibrillation[48], indicating a major susceptibility to trigger an action potential in non-nodal cardiac region. We asked if the rightward shift could be determined by a modification of the binding between HCN channels and cAMP, a cyclic nucleotide that is able to modify HCN open channel probability. After testing saturating concentration of cAMP in the pipette, a similar V_{half} value is found in all conditions as a consequence of a significant rightward shift also in the presence of the T78M in MEF-KO. This result can depend from one or more of the following reasons: 1) since the adenylyl cyclase interacts with and is inhibited by cav-3[49], in the presence of T78M cav-3 the basal concentration of cAMP in the cell could be higher; 2) the hHCN4 channels in MEF-KO cells cannot reach V_{half} values more positive than around -72 mV and thus, in the presence of the T78M cav-3 variant, we are unable to see a shift of the same magnitude as that in the presence of WT cav-3. In accordance to the Co-IP experiments, the T78M cav-3 does not affect the current density.

Even if the impact of T78M cav-3 on different channels (I_{Kur}, I_{HCN4}, $I_{Nav1.5}$ and $I_{Kir2.1}$) was demonstrated by us and others, the overall effect of the mutation on the membrane excitability is hard to predict. In order to partially overcome this point, we followed a double approach; we used NRVCs as an *in vitro* simplified cellular model of cardiomyocytes and we carried out an *in silico* analysis on atrial and sinoatrial single cells. NRVCs represent a good excitable cellular system that possess a spontaneous firing activity[40,50], and hence express all the underlying ionic currents that trigger action potential firing[51-56]. We also take advantage of the dominant negative effect exerted by T78M cav-3 in the MEF-KO system, since both an endogenous cav-3 and cav-1 are detectable in NRVCs[57]. The main advantage of this system is that it allowed us to analyze the impact of the variant not only on endogenous ionic currents, but most importantly on all the proteins residing in the caveolae[49,58]; nevertheless, it is not a model that could properly recapitulate neither the sinoatrial node nor the atrial cell.

We found that the expression of the T78M cav-3 induce a destabilization of the action potential patter (Fig. 7). Even if the average inter-beat interval (IBI) and maximum diastolic potential (MDP) were not affected, the variability of these two parameters are clearly higher in NRVCs expressing the T78M compared to the WT cav-3. The lack of the homogeneity in the cells expressing the variant could represent a substrate that could trigger arrhythmic events. Moreover, the T78M cav-3 exerted an effect also in the presence of the cav-1/cav-3 oligomers, since NRVCs possess both. However, it is important to mention that, accordingly to the rightward shift of the I_{HCN4} and I_f current showed in the presence of the T78M cav-3, the IBI should be higher in NRVCs transfected with the variant. A plausible explanation of this discordant result is that in NRVCs the I_f current density[59] is low compared to nodal systems (such as mouse[23] or rabbit sinoatrial node[60]), and hence the impact of this current on the overall firing rate could be blunted. This, as well as the absence of I_{Kur}, which is expressed in mature atrial myocytes, represent a limitation of this cellular system, . As an alternative approach to test the impact of the T78M cav-3 on the overall excitability, we carried out *in silico* analysis. We used a mathematical model of a single human atrial cell and of a rabbit sinoatrial cell (since human models of sinoatrial node cell are still lacking) since we identified the T78M cav-3 in patients affected by supraventricular arrhythmias. We modeled all the T78M-induced modifications of the ionic channels except the reduction of the I_{K1}. Indeed, the insertion of this modification lead to an action potential profile incompatible with life (Fig. 8). After testing the impact of the T78M cav-3 on $I_{Kir2.1}$ channel in MEF-KO, we indeed failed to detect any reduction, and thus we omitted this modification from the model. In the atrial cell, the simulation clearly indicate that the modifications of ionic currents triggered by T78M cav-3 produces a shortening of the action potential duration and a depolarization of the resting potential. Both effects have been previously associated with atrial fibrillation. Indeed, the depolarization of the resting potential makes atrial cells more excitable, and thus more prone to develop autorhythmic ectopic foci [61]. The shortening of the action potential decreases the relative refractory period, thus promoting the insurgence of re-entry cycle in the atrial region[41]. In sinoatrial cell, the main effect after modeling the T78M-associated modification is an increase in firing rate, perfectly compatible with the inappropriate sinus tachycardia. The main limitation of this approach is that the models represent a single cell, and hence consideration concerning the conduction of the electric signals could not be assessed. They are deterministic models, able to (and validated for) reproduce the average behavior of the cell, with fixed cycle length in the case of spontaneously beating cells. In order to reproduce inter-beat variability, more sophisticated, but less validated models including some stochastic features should be used.

Why? The impact of the study.

T78M cav-3 is the most common mutation on *CAV3* found in a broad spectrum of both skeletal and cardiac pathologies. We identified T78M cav-3 as a predisposing factor in a cohort of patient affected by supraventricular arrhythmias, thus enlarging the phenotypes associated with the T78M cav-3. The electrical phenotypic behavior showed in this and previous works describe a clear pro-arrhythmogenic effect of the variant. These data, however, were obtained using *in vitro* and *in silico* models; thus, more complex analysis (i.e. 24 hours ECG analysis and cardiac imaging) must be carried out on patients carrying the T78M cav-3. Moreover, long-term epidemiological studies in cohorts of caveolinopathy patients could shed light on the effect of cav-3 mutations in promoting cardiac electrical defects. At date, however, we need to consider that epidemiological studies argued the pathogenic role of this mutation since it could be found at a similar frequency also in the control population. The etiology of most arrhythmic diseases is complex and multifactorial, compromising genetic and environmental factors. Nowadays, pure monogenic diseases in cardiology are the exception, and not the general law. The variable penetrance in the genetic arrhythmias could be explained considering the hypothesis that genetic factors (genes that could modify the inward/outward balance of the current during action potential; i.e. *CAV3*) act as modifier of the myocardial substrate, whereas environmental factors could affect the probability and magnitude of arrhythmic-triggered events[44]. However, sorting out the effects of genetic modifiers is challenging. Demonstrating the association of a particular genetic variants with the arrhythmic syndrome requires the recruitment of a larger population. But it is not sufficient. Without additional genetic studies and functional studies, virtually all the variants in the minor-disease susceptibility genes (*CAV3, SCN4B, AKAP9, SNTA1* and *CALM3)* are uninterpretable[46]. Accordingly to the M.J. Ackerman definition, "[…] all these genes reside deep within the genetic purgatory, a place where the genetic test-ordering physician and patients and their families stuck when a variant of uncertain/unknown significance (VUS) has been elucidated". The VUS definition perfectly fits with the T78M cav-3.

How to reconcile these electrical and genetic data? Despite they appeared conflicting, they are not. Together, functional and genetic aspects shed light on the pro-arrhythmogenic contribution of the T78M cav-3 instead of its causative effect. It is reasonable to hypotize that T78M cav-3 is a genetic predisposing factor. In different cellular models, indeed, T78M cav-3 is able to trigger modifications of the ionic currents and hence of the action potential profile. Nowadays, we have not the proper cellular model to study the real impact of this variant. The

better available solution could be the use of cardiomyocytes derived from human induced-pluripotent stem cells (iPS) from patients and heathy control; in this model, we will be able to take into account all the genetic variants that could promote the onset of arrhythmias. At the same time, a better definition of the cardiological aspects in cohort of patients with mutations on cav-3 is mandatory.

Conclusions.

The T78M cav-3 variant is correctly located in the plasma membrane together with the hHCN4 and hKv1.5 channels. The kinetics properties of both channels are affected by the variant as well as overall excitability in spontaneously beating cardiomyocytes and mathematical models of atria and sinoatrial cell. The high frequency of the T78M cav-3 in a cohort of patient affected by supraventricular arrhythmias compared to our control group and ExAC database, together with our functional data, indicate a pro-arrhythmogenic contribute, even if not causative, of the T78M cav-3.

Bibliography

1 Knoll, R. A role for membrane shape and information processing in cardiac physiology. *Pflugers Archiv : European journal of physiology* **467**, 167-173, doi:10.1007/s00424-014-1575-2 (2015).

2 Sohn, J., Brick, R. M. & Tuan, R. S. From embryonic development to human diseases: The functional role of caveolae/caveolin. *Birth defects research. Part C, Embryo today : reviews* **108**, 45-64, doi:10.1002/bdrc.21121 (2016).

3 Razani, B., Woodman, S. E. & Lisanti, M. P. Caveolae: from cell biology to animal physiology. *Pharmacological reviews* **54**, 431-467 (2002).

4 Ikonen, E., Heino, S. & Lusa, S. Caveolins and membrane cholesterol. *Biochemical Society transactions* **32**, 121-123, doi:10.1042/ (2004).

5 Harvey, R. D. & Calaghan, S. C. Caveolae create local signalling domains through their distinct protein content, lipid profile and morphology. *Journal of molecular and cellular cardiology* **52**, 366-375, doi:10.1016/j.yjmcc.2011.07.007 (2012).

6 Parton, R. G. & Simons, K. The multiple faces of caveolae. *Nature reviews. Molecular cell biology* **8**, 185-194, doi:10.1038/nrm2122 (2007).

7 Busija, A. R., Patel, H. H. & Insel, P. A. Caveolins and cavins in the trafficking, maturation, and degradation of caveolae: implications for cell physiology. *American journal of physiology. Cell physiology* **312**, C459-C477, doi:10.1152/ajpcell.00355.2016 (2017).

8 Williams, T. M. & Lisanti, M. P. The caveolin proteins. *Genome biology* **5**, 214, doi:10.1186/gb-2004-5-3-214 (2004).

9 Razani, B. *et al.* Caveolin-1 null mice are viable but show evidence of hyperproliferative and vascular abnormalities. *The Journal of biological chemistry* **276**, 38121-38138, doi:10.1074/jbc.M105408200 (2001).

10 Galbiati, F. *et al.* Caveolin-3 null mice show a loss of caveolae, changes in the microdomain distribution of the dystrophin-glycoprotein complex, and t-tubule abnormalities. *The Journal of biological chemistry* **276**, 21425-21433, doi:10.1074/jbc.M100828200 (2001).

11 Park, D. S. *et al.* Caveolin-1/3 double-knockout mice are viable, but lack both muscle and non-muscle caveolae, and develop a severe cardiomyopathic phenotype. *The American journal of pathology* **160**, 2207-2217, doi:10.1016/S0002-9440(10)61168-6 (2002).

12 Balijepalli, R. C. & Kamp, T. J. Caveolae, ion channels and cardiac arrhythmias. *Progress in biophysics and molecular biology* **98**, 149-160, doi:10.1016/j.pbiomolbio.2009.01.012 (2008).

13 Balijepalli, R. C., Foell, J. D., Hall, D. D., Hell, J. W. & Kamp, T. J. Localization of cardiac L-type Ca(2+) channels to a caveolar macromolecular signaling complex is required for beta(2)-adrenergic regulation. *Proceedings of the National Academy of Sciences of the United States of America* **103**, 7500-7505, doi:10.1073/pnas.0503465103 (2006).

14 Harvey, R. D. & Hell, J. W. CaV1.2 signaling complexes in the heart. *Journal of molecular and cellular cardiology* **58**, 143-152, doi:10.1016/j.yjmcc.2012.12.006 (2013).

15 Calaghan, S. & White, E. Caveolae modulate excitation-contraction coupling and beta2-adrenergic signalling in adult rat ventricular myocytes. *Cardiovascular research* **69**, 816-824, doi:10.1016/j.cardiores.2005.10.006 (2006).

16 Balijepalli, R. C. *et al.* Kv11.1 (ERG1) K+ channels localize in cholesterol and sphingolipid enriched membranes and are modulated by membrane cholesterol. *Channels* **1**, 263-272 (2007).

17 McEwen, D. P., Li, Q., Jackson, S., Jenkins, P. M. & Martens, J. R. Caveolin regulates kv1.5 trafficking to cholesterol-rich membrane microdomains. *Molecular pharmacology* **73**, 678-685, doi:10.1124/mol.107.042093 (2008).

18 Folco, E. J., Liu, G. X. & Koren, G. Caveolin-3 and SAP97 form a scaffolding protein complex that regulates the voltage-gated potassium channel Kv1.5. *American journal of physiology. Heart and circulatory physiology* **287**, H681-690, doi:10.1152/ajpheart.00152.2004 (2004).

19 Martens, J. R., Sakamoto, N., Sullivan, S. A., Grobaski, T. D. & Tamkun, M. M. Isoform-specific localization of voltage-gated K+ channels to distinct lipid raft populations. Targeting of Kv1.5 to caveolae. *The Journal of biological chemistry* **276**, 8409-8414, doi:10.1074/jbc.M009948200 (2001).

20 Brown, H., Difrancesco, D. & Noble, S. Cardiac pacemaker oscillation and its modulation by autonomic transmitters. *The Journal of experimental biology* **81**, 175-204 (1979).
21 DiFrancesco, D. The role of the funny current in pacemaker activity. *Circulation research* **106**, 434-446, doi:10.1161/CIRCRESAHA.109.208041 (2010).
22 DiFrancesco, D. & Tortora, P. Direct activation of cardiac pacemaker channels by intracellular cyclic AMP. *Nature* **351**, 145-147, doi:10.1038/351145a0 (1991).
23 Barbuti, A. *et al.* Localization of pacemaker channels in lipid rafts regulates channel kinetics. *Circulation research* **94**, 1325-1331, doi:10.1161/01.RES.0000127621.54132.AE (2004).
24 Barbuti, A., Terragni, B., Brioschi, C. & DiFrancesco, D. Localization of f-channels to caveolae mediates specific beta2-adrenergic receptor modulation of rate in sinoatrial myocytes. *Journal of molecular and cellular cardiology* **42**, 71-78, doi:10.1016/j.yjmcc.2006.09.018 (2007).
25 Barbuti, A. *et al.* A caveolin-binding domain in the HCN4 channels mediates functional interaction with caveolin proteins. *Journal of molecular and cellular cardiology* **53**, 187-195, doi:10.1016/j.yjmcc.2012.05.013 (2012).
26 Bruno, C., Sotgia, F., Gazzerro, E., Minetti, C. & Lisanti, M. P. in *GeneReviews(R)* (eds M. P. Adam *et al.*) (1993).
27 Gazzerro, E., Sotgia, F., Bruno, C., Lisanti, M. P. & Minetti, C. Caveolinopathies: from the biology of caveolin-3 to human diseases. *European journal of human genetics : EJHG* **18**, 137-145, doi:10.1038/ejhg.2009.103 (2010).
28 Hedley, P. L. *et al.* The role of CAV3 in long-QT syndrome: clinical and functional assessment of a caveolin-3/Kv11.1 double heterozygote versus caveolin-3 single heterozygote. *Circulation. Cardiovascular genetics* **6**, 452-461, doi:10.1161/CIRCGENETICS.113.000137 (2013).
29 Gazzerro, E., Bonetto, A. & Minetti, C. Caveolinopathies: translational implications of caveolin-3 in skeletal and cardiac muscle disorders. *Handbook of clinical neurology* **101**, 135-142, doi:10.1016/B978-0-08-045031-5.00010-4 (2011).
30 Vatta, M. *et al.* Mutant caveolin-3 induces persistent late sodium current and is associated with long-QT syndrome. *Circulation* **114**, 2104-2112, doi:10.1161/CIRCULATIONAHA.106.635268 (2006).
31 Cronk, L. B. *et al.* Novel mechanism for sudden infant death syndrome: persistent late sodium current secondary to mutations in caveolin-3. *Heart rhythm* **4**, 161-166, doi:10.1016/j.hrthm.2006.11.030 (2007).
32 Ricci, G. *et al.* Rippling muscle disease and facioscapulohumeral dystrophy-like phenotype in a patient carrying a heterozygous CAV3 T78M mutation and a D4Z4 partial deletion: Further evidence for "double trouble" overlapping syndromes. *Neuromuscular disorders : NMD* **22**, 534-540, doi:10.1016/j.nmd.2011.12.001 (2012).
33 Traverso, M. *et al.* Caveolin-3 T78M and T78K missense mutations lead to different phenotypes in vivo and in vitro. *Laboratory investigation; a journal of technical methods and pathology* **88**, 275-283, doi:10.1038/labinvest.3700713 (2008).
34 Vaidyanathan, R. *et al.* The interaction of caveolin 3 protein with the potassium inward rectifier channel Kir2.1: physiology and pathology related to long qt syndrome 9 (LQT9). *The Journal of biological chemistry* **288**, 17472-17480, doi:10.1074/jbc.M112.435370 (2013).
35 Refsgaard, L. *et al.* High prevalence of genetic variants previously associated with LQT syndrome in new exome data. *European journal of human genetics : EJHG* **20**, 905-908, doi:10.1038/ejhg.2012.23 (2012).
36 Andreasen, C. *et al.* Mutations in genes encoding cardiac ion channels previously associated with sudden infant death syndrome (SIDS) are present with high frequency in new exome data. *The Canadian journal of cardiology* **29**, 1104-1109, doi:10.1016/j.cjca.2012.12.002 (2013).
37 Spadafora, P., Liguori, M., Andreoli, V., Quattrone, A. & Gambardella, A. CAV3 T78M mutation as polymorphic variant in South Italy. *Neuromuscular disorders : NMD* **22**, 669-670; author reply 670-661, doi:10.1016/j.nmd.2012.03.007 (2012).
38 Grandi, E. *et al.* Human atrial action potential and Ca2+ model: sinus rhythm and chronic atrial fibrillation. *Circulation research* **109**, 1055-1066, doi:10.1161/CIRCRESAHA.111.253955 (2011).

39 Koivumaki, J. T., Korhonen, T. & Tavi, P. Impact of sarcoplasmic reticulum calcium release on calcium dynamics and action potential morphology in human atrial myocytes: a computational study. *PLoS computational biology* **7**, e1001067, doi:10.1371/journal.pcbi.1001067 (2011).
40 Baruscotti, M. *et al.* A gain-of-function mutation in the cardiac pacemaker HCN4 channel increasing cAMP sensitivity is associated with familial Inappropriate Sinus Tachycardia. *European heart journal* **38**, 280-288, doi:10.1093/eurheartj/ehv582 (2017).
41 Heijman, J., Voigt, N., Nattel, S. & Dobrev, D. Cellular and molecular electrophysiology of atrial fibrillation initiation, maintenance, and progression. *Circulation research* **114**, 1483-1499, doi:10.1161/CIRCRESAHA.114.302226 (2014).
42 Ackerman, M. J. & Mohler, P. J. Defining a new paradigm for human arrhythmia syndromes: phenotypic manifestations of gene mutations in ion channel- and transporter-associated proteins. *Circulation research* **107**, 457-465, doi:10.1161/CIRCRESAHA.110.224592 (2010).
43 Wang, Q. *et al.* SCN5A mutations associated with an inherited cardiac arrhythmia, long QT syndrome. *Cell* **80**, 805-811 (1995).
44 Schwartz, P. J., Ackerman, M. J., George, A. L., Jr. & Wilde, A. A. Impact of genetics on the clinical management of channelopathies. *Journal of the American College of Cardiology* **62**, 169-180, doi:10.1016/j.jacc.2013.04.044 (2013).
45 Nassoy, P. & Lamaze, C. Stressing caveolae new role in cell mechanics. *Trends Cell Biol* **22**, 381-389, doi:10.1016/j.tcb.2012.04.007 (2012).
46 Ackerman, M. J. Genetic purgatory and the cardiac channelopathies: Exposing the variants of uncertain/unknown significance issue. *Heart rhythm* **12**, 2325-2331, doi:10.1016/j.hrthm.2015.07.002 (2015).
47 Olson, T. M. *et al.* Kv1.5 channelopathy due to KCNA5 loss-of-function mutation causes human atrial fibrillation. *Human molecular genetics* **15**, 2185-2191, doi:10.1093/hmg/ddl143 (2006).
48 Stillitano, F. *et al.* Chronic atrial fibrillation alters the functional properties of If in the human atrium. *Journal of cardiovascular electrophysiology* **24**, 1391-1400, doi:10.1111/jce.12212 (2013).
49 Rybin, V. O., Xu, X., Lisanti, M. P. & Steinberg, S. F. Differential targeting of beta -adrenergic receptor subtypes and adenylyl cyclase to cardiomyocyte caveolae. A mechanism to functionally regulate the cAMP signaling pathway. *The Journal of biological chemistry* **275**, 41447-41457, doi:10.1074/jbc.M006951200 (2000).
50 de Boer, T. P. *et al.* Inhibition of cardiomyocyte automaticity by electrotonic application of inward rectifier current from Kir2.1 expressing cells. *Medical & biological engineering & computing* **44**, 537-542, doi:10.1007/s11517-006-0059-8 (2006).
51 Shi, W. *et al.* Distribution and prevalence of hyperpolarization-activated cation channel (HCN) mRNA expression in cardiac tissues. *Circulation research* **85**, e1-6 (1999).
52 He, Y. *et al.* Kir2.3 knock-down decreases IK1 current in neonatal rat cardiomyocytes. *FEBS letters* **582**, 2338-2342, doi:10.1016/j.febslet.2008.05.023 (2008).
53 Guo, W., Kada, K., Kamiya, K. & Toyama, J. IGF-I regulates K(+)-channel expression of cultured neonatal rat ventricular myocytes. *The American journal of physiology* **272**, H2599-2606 (1997).
54 Guo, J. *et al.* Identification of IKr and its trafficking disruption induced by probucol in cultured neonatal rat cardiomyocytes. *The Journal of pharmacology and experimental therapeutics* **321**, 911-920, doi:10.1124/jpet.107.120931 (2007).
55 Gomez, J. P., Potreau, D., Branka, J. E. & Raymond, G. Developmental changes in Ca2+ currents from newborn rat cardiomyocytes in primary culture. *Pflugers Archiv : European journal of physiology* **428**, 241-249 (1994).
56 Kaufmann, S. G. *et al.* Functional protein expression of multiple sodium channel alpha- and beta-subunit isoforms in neonatal cardiomyocytes. *Journal of molecular and cellular cardiology* **48**, 261-269, doi:10.1016/j.yjmcc.2009.04.017 (2010).
57 Lal, H. *et al.* Caveolin and beta1-integrin coordinate angiotensinogen expression in cardiac myocytes. *International journal of cardiology* **168**, 436-445, doi:10.1016/j.ijcard.2012.09.131 (2013).
58 Rybin, V. O., Xu, X. & Steinberg, S. F. Activated protein kinase C isoforms target to cardiomyocyte caveolae : stimulation of local protein phosphorylation. *Circulation research* **84**, 980-988 (1999).

59 Avitabile, D. *et al.* Human cord blood CD34+ progenitor cells acquire functional cardiac properties through a cell fusion process. *American journal of physiology. Heart and circulatory physiology* **300**, H1875-1884, doi:10.1152/ajpheart.00523.2010 (2011).

60 Baruscotti, M. *et al.* Deep bradycardia and heart block caused by inducible cardiac-specific knockout of the pacemaker channel gene Hcn4. *Proceedings of the National Academy of Sciences of the United States of America* **108**, 1705-1710, doi:10.1073/pnas.1010122108 (2011).

61 Wakili, R., Voigt, N., Kaab, S., Dobrev, D. & Nattel, S. Recent advances in the molecular pathophysiology of atrial fibrillation. *The Journal of clinical investigation* **121**, 2955-2968, doi:10.1172/JCI46315 (2011).